Supporting Information

Facile Multicomponent Polymerizations toward Unconventional Luminescent Polymers with Readily Openable Small Heterocycles

Ting Han,[†,‡,#] Haiqin Deng,[†,‡,#] Zijie Qiu,[†,‡] Zheng Zhao,[†,‡] Haoke Zhang,[†,‡] Hang Zou,[†,‡] Nelson L. C. Leung,[†,‡] Guogang Shan,[†,‡] Mark R. J. Elsegood,[¶] Jacky W. Y. Lam,*[,†,‡] and Ben Zhong Tang*[,†,‡,§]

[†]Department of Chemistry, Hong Kong Branch of Chinese National Engineering Research Center for Tissue Restoration and Reconstruction, Institute for Advanced Study, Division of Biomedical Engineering and Division of Life Science, The Hong Kong University of Science and Technology, Clear Water Bay, Kowloon, Hong Kong, China

[‡]HKUST-Shenzhen Research Institute, No. 9 Yuexing 1st RD, South Area, Hi-tech Park, Nanshan, Shenzhen 518057, China

[§]China NSFC Center for Luminescence from Molecular Aggregates, SCUT-HKUST Joint Research Institute, State Key Laboratory of Luminescent Materials and Devices, South China University of Technology, Guangzhou 510640, China

[¶]Chemistry Department, Loughborough University, Loughborough, Leicestershire, LE11 3TU, UK

Table of Contents

Materials and Methods

N,*N'*-Dicyclohexylcarbodiimide, *N*,*N'*-diisopropylcarbodiimide, CuI, phenylacetylene, and all other chemicals and reagents were purchased from Meryer, J&K Scientific, Aldrich, or Merck and used as commercially received unless stated otherwise. Dichromethane (DCM) and tetrahydrofuran (THF) were distilled under nitrogen and normal pressure from CaH_2 and sodium/benzophenone, respectively, and degassed before use. Diyne **1a** was obtained from AIEgen Biotech Co., Ltd. diynes **1b**–**c**, disulfonyl azide **2a**–**c**, and *p*-toluenesulfonyl azide were prepared according to the previous reported procedures.[1]

Weight- (M_w) and number-average molecular weights (M_n) and polydispersity indices (M_w/M_n) of the obtained polymers were estimated on a Waters gel permeation chromatography (GPC) system equipped with a UV detector and calibrated using a set of monodispersed polystyrene standards. THF was used as an eluent. Details about the sample preparation and experimental setup can be found in our previous publications.[2] FT-IR spectra and high-resolution mass spectra (HRMS) were recorded on a Bruker Vertex 70 FT-IR spectrometer (KBr disk) and a GCT Premier CAB 048 mass spectrometer, respectively. ^{1}H and ^{13}C NMR spectra were obtained on a Bruker ARX 400 NMR spectrometer using $CDCl_3$ as a solvent. Chemical shifts were calibrated using $CDCl_3$ as internal reference at δ 7.26 ppm (^{1}H NMR) and δ 77.16 ppm (^{13}C NMR). TGA and DSC measurements were carried on a TA TGA Q5000 and a TA Instruments DSC Q1000, respectively, at a heating rate of 10 °C/min under nitrogen. UV-vis spectra and PL spectra were measured on a Milton Ray Spectronic 3000 Array spectrophotometer and a PerkinElmer LS 55 spectrophotometer, respectively. XPS measurements were performed with a Physical Electronics 5600 multi-technique system and the C 1s peak was shifted to 285.0 eV for energy calibration. The size and morphology of the prepared nanoparticles were measured on a Brookhaven Zeta potential analyzer and a JEOL-6700F Scanning Electron Microscopy (SEM) with a model of JSM-6700F, respectively. RI values were determined on a Woollam ellipsometer with a model of Alpha-SE with a wavelength tunability from 390 to 890 nm. The fluorescent photopatterns were taken on a fluorescence optical microscope (Nikon Eclipse 80i) under a UV light source (330–380 nm). Thin films for RI measurement were fabricated by spin-coating the 1,2-dichloroethane solutions of the polymers (~10 mg mL^{-1}) on silicon wafers at 700 rpm for 1 min, and then dried in a vacuum oven at room temperature overnight. The photopatterns were generated by UV irradiating the polymer thin films through a photomask for 20 min in air at room temperature.

The photomask used herein was a grid pattern, in which the square areas were opaque and coated with copper whereas the grid lines were transparent glass substrate. The photo-irradiation process was conducted using UV light from an Oriel Mercury Arc Lamp at a distance of 25 cm. The incident light intensity was ~18.5 mW cm^{-2} and the applied power of the Mercury Arc Lamp was 180 W.

Preparation of Polymer and Model Compound Nanoparticles: 1 mL THF solution containing 1.0 mg polymer or model compound and 2.0 mg DSPE-PEG_{2000} was slowly added into 10 mL distilled water under sonication by Qsonica Q125 sonicator with 20% output for 4 min. The mixture was then concentrated to 1 mL by blowing with condensed air under stirring at room temperature, during which the THF solvent was removed at the same time. After filtration with 0.2 μm filter, the final residue was used as a stock solution of nanoparticles (NPs) for the following experiments.

Cell Culture and Imaging: HeLa cells were cultured in DMEM medium containing 10% FBS and antibiotics (100 units/mL penicillin and 100 μg/mL streptomycin) in a humidified environment of 5% CO_2 at 37 °C. After incubated for 12 h, the medium was removed by washing the adherent cells with PBS buffer for three times. Then 240 μL of the pre-prepared stock solution of polymer NPs with a concentration of 1 mg/mL was added into 2 mL culture medium. Subsequently, the live cells were stained with such medium for 18 h followed by LysoTracker Red DND-99 (LTR) with a concentration of 50 nM for 10 min. The excess dye was washed away with PBS buffer. A confocal microscope (Zeiss, LSM7 DUO) using ZEN 2009 software (Carl Zeiss) was used to image the HeLa cells. The photostability of P**5** NPs was measured by exciting the sample at 405 nm with 2% laser power. The fluorescence was collected at 410–509 nm.

The cytotoxicity of P**5** NPs on HeLa cells was evaluated using 3-(4,5-dimethyl-2-thiazolyl)-2,5-diphenyltetrazolium bromide (MTT) assay.[3] The cell viability was assayed by cell proliferation Kit I and the absorbance at 595 nm was detected by a Perkin-Elmer Victor plate reader. The cells were seeded in a 96-well plate at a density of 4000 cells per well. After overnight culturing, P**5** NPs with different concentrations were then added to this 96-well plate and treated for 24 h. Then 10 μL of MTT solution (5 mg/mL in phosphate buffer solution) was added into each well. After incubation at 37 °C for 4 h, the MTT medium solution was removed carefully and 100 μL of DMSO was added to dissolve the purple crystals. After 20 min of incubation, the absorbance of MTT at 595 nm was recorded by a plate reader (Perkin-Elmer Victor 3). The cell viability was represented by the ratio of absorbance of the

cells incubated with various concentrations of polymer NPs to that of cells incubated with culture medium only. Each of the experiments was performed at least 3 times.

The stability of the prepared polymers under normal room light was tested by irradiating the polymer thin films by light from a LED daylight lamp (product model: LED-BPZ220/3.5-E27-5) with a power of 3.5 W at a distance of ~15 cm. This experiment was conducted in a darkroom to minimize the interferences from other light sources. Taking P**1a**/**2a**/**3a** as an example, the prepared polymer thin films were irradiated by the LED daylight lamp for 24 h and 7 days, respectively. The UV spectra of the thin films before and after light irradiation were measured. The ^{1}H NMR spectra of the thin films after light irradiation were also checked by washing the film sample using $CDCl_3$. After solvent evaporation, the obtained samples were then collected for IR measurement. No obvious signal change was observed in the obtained ^{1}H NMR, IR and UV spectra of the polymer samples after light irradiation, which indicated the good stability of the polymers under normal room light.

Synthesis and Characterization

Model Reaction: To a 10 mL Schlenk tube were placed a magnetic stirrer, *p*-toluenesulfonyl azide (197 mg, 1.0 mmol), *N*,*N'*-dicyclohexylcarbodiimide (247 mg, 1.2 mmol), and CuI (19 mg, 0.1 mmol). Then anhydrous DCM (3 mL) and phenylacetylene (102 mg, 1.0 mmol) were slowly injected into the system under N_2. The resulting mixture was stirred for 17 h at room temperature. After solvent removal, the crude residue was purified by silica-gel column chromatography using ethyl acetate/*n*-hexane mixture (1/7, v/v) as eluent. After recrystallization from DCM/*n*-hexane mixture, pure product was obtained as a white solid in a yield of 60.6%. IR (KBr), ν (cm^{-1}): 3045, 2936, 2855, 1761, 1612, 1316, 1159. ^{1}H NMR (400 MHz, $CDCl_3$), δ (ppm): 7.33–7.26 (m, 3H), 7.19 (d, J = 8.0 Hz, 2H), 7.09 (d, J = 8.0 Hz, 2H), 6.98 (d, J = 8.0 Hz, 2H), 5.26 (s, 1H), 3.85–3.77 (m, 1H), 2.99–2.92 (m, 1H), 2.32 (s, 3H), 2.09–0.78 (m, 20H). ^{13}C NMR (100 MHz, $CDCl_3$), δ (ppm): 167.03, 151.34, 142.75, 138.41, 132.33, 129.04, 128.28, 126.77, 60.75, 58.91, 53.20, 34.64, 33.60, 29.86, 29.78, 25.53, 25.32, 24.96, 24.58, 24.42, 21.58. HRMS (CI, NH_3): m/z $[M + H]^+$ calcd for $C_{28}H_{36}N_3O_2S$, 477.2450; found, 478.2528.

Polymer Synthesis: Standard Schlenk technique was applied in all the polymerization reactions and the synthetic procedure of P**1a**/**2a**/**3a** (Table 1, entry 3) was given below as an example. Into a 10 mL Schlenk tube with a two-way stopcock on the sidearm were added TPE-containing diyne **1a** (76.1 mg, 0.20 mmol), disulfonyl azide **2a** (76.1 mg, 0.20 mmol), *N*,*N'*-dicyclohexylcarbodiimide (99.0 mg, 0.48 mmol), and CuI (7.6 mg, 0.04 mmol). Then 0.50 mL of distilled DCM was injected under nitrogen protection. After stirring for 24 h at room temperature in a sealed tube, the polymerization was stopped. The resulting solution was diluted with 3 mL of DCM and then added dropwisely into 200 mL of $CHCl_3$/*n*-hexane mixture (1/10) through a neutral Al_2O_3-filled dropper to remove the catalyst residue. The precipitate was finally collected after filtration, washing with *n*-hexane and dried under vacuum at room temperature to a constant weight. The structural characterization results were summarized as follows.

*Characterization Data for P**1a/2a/3a***: Light yellow powder; 80.9% (Table 1, entry 3). M_n: 9000; M_w: 24500; M_w/M_n: 2.7 (GPC, polystyrene calibration). IR (KBr), ν (cm^{-1}): 3025, 2931, 2856, 1762, 1614, 1488, 1325, 1245, 1157. ^{1}H NMR (400 MHz, $CDCl_3$), δ (ppm): 7.43, 7.06–6.88 (aromatic protons), 5.15 (CH protons), 3.75 (CH protons), 2.96 (CH protons), 1.98, 1.83, 1.74, 1.20, 0.94. ^{13}C NMR (100 MHz, $CDCl_3$), δ (ppm): 166.94, 159.27, 151.02, 143.65, 143.22, 140.70,

140.51, 137.02, 131.78–126.79, 118.83, 60.62, 58.71, 53.22, 34.60, 33.54, 29.76, 25.58, 25.52, 24.92, 24.64, 24.51.

*Characterization Data for P**1a/2a/3b***: Light yellow powder; 83.5% (Table 1, entry 7). M_n: 11000; M_w: 74500; M_w/M_n: 6.8 (GPC, polystyrene calibration). IR (KBr), ν (cm^{-1}): 3025, 2972, 2935, 2873, 1762, 1614, 1486, 1324, 1245, 1157. ^1H NMR (400 MHz, $CDCl_3$), δ (ppm): 7.37, 7.00–6.79 (aromatic protons), 5.16 (CH protons), 4.14 (CH protons), 3.26 (CH protons), 1.41, 1.07, 0.66. ^{13}C NMR (100 MHz, $CDCl_3$), δ (ppm): 166.64, 159.28, 150.67, 143.65, 143.01, 140.97, 140.51, 136.88, 131.68–126.94, 118.78, 60.66, 50.95, 45.92, 24.60, 23.68, 20.01.

*Characterization Data for P**1b/2a/3a***: Yellowish-white powder; 76.4% (Table 1, entry 8). M_n: 5000; M_w: 10200; M_w/M_n: 2.0 (GPC, polystyrene calibration). IR (KBr), ν (cm^{-1}): 3031, 2931, 2856, 1763, 1615, 1488, 1324, 1245, 1157. ^1H NMR (400 MHz, $CDCl_3$), δ (ppm): 7.51, 7.42, 7.36, 7.32, 7.28, 6.78, 6.71, 5.30, 3.83, 3.02, 2.05, 1.93, 1.81, 1.66, 1.43, 1.08, 0.95. ^{13}C NMR (100 MHz, $CDCl_3$), δ (ppm): 167.28, 159.15, 150.72, 140.24, 137.14, 132.82, 131.80, 130.23, 129.13, 128.78, 127.44, 126.86, 118.95, 60.56, 58.83, 53.34, 34.58, 33.63, 29.83, 25.46, 25.29, 24.94, 24.46, 24.32.

*Characterization Data for P**1c/2a/3a***: White powder; 78.9% (Table 1, entry 9). M_n: 9400; M_w: 29200; M_w/M_n: 3.1 (GPC, polystyrene calibration). IR (KBr), ν (cm^{-1}): 3041, 2931, 2856, 1765, 1616, 1510, 1488, 1316, 1244, 1157. ^1H NMR (400 MHz, $CDCl_3$), δ (ppm): 7.83, 7.81, 7.08, 7.06, 6.91, 6.89, 6.71, 6.69, 4.73, 4.71, 4.53, 4.37, 4.35, 3.74, 3.26, 2.00, 1.97, 1.84, 1.75, 1.65, 1.47, 1.21, 1.19. ^{13}C NMR (100 MHz, $CDCl_3$), δ (ppm): 166.44, 159.20, 155.84, 148.59, 144.01, 137.36, 128.97, 127.87, 118.99, 114.11, 63.54, 59.10, 56.66, 53.13, 41.84, 34.85, 34.36, 31.09, 29.53, 29.45, 25.60, 25.26, 25.00, 24.64, 24.58.

*Characterization Data for P**1a/2b/3a***: Light yellow powder; 47.9% (Table 1, entry 10). M_n: 6100; M_w: 9000; M_w/M_n: 1.5 (GPC, polystyrene calibration). IR (KBr), ν (cm^{-1}): 3058, 2934, 2856, 1763, 1615, 1514, 1321, 1161. ^1H NMR (400 MHz, $CDCl_3$), δ (ppm): 7.49, 7.04–6.90 (aromatic protons), 5.18 (CH protons), 3.77 (CH protons), 2.97 (CH protons), 2.00, 1.85, 1.75, 1.59, 1.20, 0.96. ^{13}C NMR (100 MHz, $CDCl_3$), δ (ppm): 167.15, 150.74, 143.67, 143.47, 141.54, 141.41, 141.32, 140.95, 140.67, 131.83, 131.28, 128.84, 128.51, 128.09, 127.59, 127.38, 127.04, 60.81, 58.66, 53.40, 34.67, 33.63, 29.82, 25.65, 25.31, 25.00, 24.63, 24.49.

*Characterization Data for P**1a/2c/3a***: Light yellow powder; 72.4% (Table 1, entry 11). M_n: 7900; M_w: 13800; M_w/M_n: 1.7 (GPC, polystyrene calibration). IR (KBr), ν (cm^{-1}): 3062, 2929,

2856, 1763, 1608, 1503, 1414, 1325, 1152. ^{1}H NMR (400 MHz, $CDCl_3$), δ (ppm): 7.41, 7.08–6.83 (aromatic protons), 5.13 (CH protons), 3.77 (CH protons), 2.97 (CH protons), 1.96, 1.84, 1.76, 1.60, 1.22, 0.92. ^{13}C NMR (100 MHz, $CDCl_3$), δ (ppm): 167.51, 151.12, 143.54, 143.04, 142.04, 139.99, 139.17, 131.97, 131.76, 130.98, 130.49, 130.14, 129.36, 127.98, 127.39, 127.04, 60.75, 58.84, 53.45, 34.51, 33.51, 29.73, 25.51, 25.19, 24.86, 24.59, 24.49.

*Ring-Opening Reaction of **4***: The solution of model compound **4** (239 mg, 0.5 mmol) dissolved in 3 mL THF was placed in a 10 mL Schlenk tube, and 0.05 mL of 37 wt % aqueous HCl solution was then slowly added. The resulting mixture was stirred for about 40 min at room temperature. Then the mixture was neutralized by aqueous $NaHCO_3$ solution, followed by extraction with DCM for three times. Subsequently, the organic layer was collected and concentrated and the crude product was purified by silica-gel column chromatography using ethyl acetate/*n*-hexane mixture (1/6, v/v) as eluent. Pure product **5** was obtained as a white solid in a yield of 90.6%. Single crystals of **5** were grown by vapor diffusion of *n*-hexane into its DCM solution. IR (KBr), ν (cm^{-1}): 3307, 3063, 2935, 2853, 1661, 1570, 1536, 1450, 1271, 1135, 1087. ^{1}H NMR (400 MHz, $CDCl_3$), δ (ppm): 7.92 (d, J = 8.0 Hz, 1H), 7.65 (d, J = 8.0 Hz, 2H), 7.38–7.36 (m, 2H), 7.29–7.25 (m, 3H), 7.15 (d, J = 8.0 Hz, 2H), 6.40 (d, J = 8.0 Hz, 1H), 5.77 (s, 1H), 3.84–3.93 (m, 1H), 3.73–3.64 (m, 1H), 2.36 (s, 3H), 1.87–1.06 (m, 20H). ^{13}C NMR (100 MHz, $CDCl_3$), δ (ppm): 167.03, 151.34, 142.75, 138.41, 132.33, 129.04, 128.28, 126.77, 60.75, 58.91, 53.20, 34.64, 33.60, 29.86, 29.78, 25.53, 25.32, 24.96, 24.58, 24.42, 21.58. 168.70, 161.87, 142.03, 140.88, 135.16, 129.14, 128.94, 128.02, 127.96, 126.18, 52.62, 50.39, 49.28, 32.52, 32.49, 31.67, 31.62, 25.55, 25.42, 24.90, 24.83, 24.30, 21.54. HRMS (MALFI-TOF): m/z 496.2644 ([M + H]$^+$, calcd 496.2634), 518.2622 ([M + Na]$^+$, calcd 518.2453), 534.2313 ([M+K]$^+$, calcd 534.2193) (Figure S4 in the Supporting Information). Anal. calcd for $C_{28}H_{37}N_3O_3S$: C 67.85, H 7.52, N 8.48; found: C 67.98, H 7.55, N 8.48.

Ring-Opening Reaction of Polymers: The experimental procedure of the ring-opening reaction was given below with P**1a**/**2a**/**3a** as an example. Into a 10 mL Schlenk tube were added the solution of P**1a**/**2a**/**3a** (56 mg, 0.05 mmol) dissolved in 1 mL THF. Then 0.2 mL of 37 wt % aqueous HCl solution was slowly added and the mixture was stirred for 1 h at room temperature. After neutralization by $NaHCO_3$ aqueous solution, extraction with DCM for three times and the subsequent concentration of the organic layer, the resulting solution was added dropwisely into 200 mL of $CHCl_3$/*n*-hexane mixture (1/10) for precipitation. The precipitate was collected by filtration, washing with *n*-hexane and dried under vacuum overnight.

*Characterization Data for P**5***: Light yellow powder. M_n: 7600; M_w: 12100; M_w/M_n: 1.6 (GPC, polystyrene calibration;sample obtained from the ring-opening reaction of P**1a**/**2a**/**3a** with a M_n of 6700, a M_w of 10300 and a M_w/M_n of 1.5). IR (KBr), ν (cm^{-1}): 3402, 3058, 2932, 2855, 1665, 1567, 1488, 1450, 1245, 1143, 1090. ^{1}H NMR (400 MHz, $CDCl_3$), δ (ppm): 7.84, 7.16–6.94, 5.69, 3.82, 3.66, 1.80–1.14. ^{13}C NMR (100 MHz, $CDCl_3$), δ (ppm): 168.49, 162.23, 158.88, 143.36, 140.86, 139.43, 133.61, 131.86–126.75, 118.79, 52.60, 50.40, 49.23, 32.40, 31.49, 25.51, 24.89, 24.18.

*Characterization Data for P**6***: Light yellow powder. M_n: 5000; M_w: 8100; M_w/M_n: 1.6 (GPC, polystyrene calibration; sample obtained from the ring-opening reaction of P**1b**/**2a**/**3a** with a M_n of 4500, a M_w of 7800 and a M_w/M_n of 1.7). IR (KBr), ν (cm^{-1}): 3314, 3071, 2931, 2854, 1664, 1567, 1489, 1450, 1245, 1143, 1089. ^{1}H NMR (400 MHz, $CDCl_3$), δ (ppm): 7.83, 7.64–7.31, 7.08–7.00, 6.30, 5.78, 3.92, 3.70, 1.91–1.13. ^{13}C NMR (100 MHz, $CDCl_3$), δ (ppm): 168.70, 162.03, 158.61, 140.75, 139.88, 132.75, 130.26, 128.56, 127.59, 126.98, 119.73. 118.89, 52.46, 50.67, 49.46, 32.60, 32.35, 31.64, 25.52, 24.94, 24.31.

*Characterization Data for P**7***: White powder. M_n: 6000; M_w: 9700; M_w/M_n: 1.6 (GPC, polystyrene calibration; sample obtained from the ring-opening reaction of P**1c**/**2a**/**3a** with a M_n of 6800, a M_w of 12800 and a M_w/M_n of 1.9). IR (KBr), ν (cm^{-1}): 3317, 3071, 2931, 2854, 1664, 1562, 1510, 1488, 1449, 1245, 1143, 1089. ^{1}H NMR (400 MHz, $CDCl_3$), δ (ppm): 7.92, 7.12–6.97, 6.85, 6.68, 4.82, 4.31, 4.24, 3.82, 3.73, 1.84–1.21. ^{13}C NMR (100 MHz, $CDCl_3$), δ (ppm): 167.71, 160.93, 158.96, 155.88, 144.02, 139.18, 128.72, 127.85, 118.96, 114.36, 68.18, 50.58, 49.23, 48.69, 41.87, 32.63, 32.47, 31.66, 31.42, 31.12, 25.48, 24.77, 24.28.

Table S1. Effect of monomer concentration on the polymerizations of 1a, 2a and 3a[a]

entry	[**1a**] (M)	yield (%)	M_n[b]	M_w[b]	$Đ$[b]
1	0.10	39.8	2500	3200	1.3
2	0.20	70.3	3800	6100	1.6
3	0.30	78.0	6900	12900	1.9
4	0.40	80.9	9000	24500	2.7

[a] Carried out at room temperature under nitrogen in CH_2Cl_2 for 24 h, [**1a**] = [**2a**], [**3a**] = 2.4 [**1a**], [CuI] = 20 mol%. [b] Estimated by GPC in THF on the basis of a linear polystyrene calibration. $Đ$ = polydispersity = M_w/M_n.

Table S2. Solvent effect on the polymerizations of 1a, 2a and 3a[a]

entry	solvent	yield (%)	M_n[b]	M_w[b]	$Đ$[b]
1[c]	CH_2Cl_2	80.9	9000	24500	2.7
2	THF	80.0	5800	12900	2.2
3	$CHCl_3$	84.6	6400	16400	2.6
4[d]	DMAc	gel			

[a] Carried out at room temperature under nitrogen for 24 h, [**1a**] = [**2a**] = 0.40 M, [**3a**] = 0.96 M, [CuI] = 20 mol%. Entries 1-3 were also provided in Table 1 as representative examples. [b] Estimated by GPC in THF on the basis of a linear polystyrene calibration. $Đ$ = polydispersity = M_w/M_n. [c] Data taken from Table S1, entry 4. [d] DMAc = dimethylacetamide. The GPC data for the soluble fraction was M_n = 8700, M_w = 32500 and $Đ$ = 3.7

Table S3. Time course on the polymerizations of 1a, 2a and 3a[a]

entry	t (h)	yield (%)	M_n[b]	M_w[b]	$Đ$[b]
1	6	24.2	1800	2200	1.2
2	12	57.2	2900	4300	1.5
3	18	70.7	5700	9600	1.7
4[c]	24	80.9	9000	24500	2.7
5	27	83.2	9000	42500	4.7

[a] Carried out at room temperature under nitrogen in CH_2Cl_2, [**1a**] = [**2a**] = 0.40 M, [**3a**] = 0.96 M, [CuI] = 20 mol%. [b] Estimated by GPC in THF on the basis of a linear polystyrene calibration. $Đ$ = polydispersity = M_w/M_n. [c] Data taken from Table S1, entry 4.

Table S4. Effect of temperature on the polymerizations of 1a, 2a and 3a[a]

entry	T (°C)	yield (%)	M_n[b]	M_w[b]	M_w/M_n[b]
1	0	~0[c]			
2[d]	25	81.3	8100	21600	2.7
3[e]	40	84.6	9100	23500	2.6

[a] Carried out in CH_2Cl_2 under nitrogen for 24 h, [**1a**] = [**2a**] = 0.40 M, [**3a**] = 0.96 M, [CuI] = 10 mol%. [b] Estimated by GPC in THF on the basis of a linear polystyrene calibration. $Đ$ = polydispersity = M_w/M_n. [c] No reacton. [d] Data taken from Table 1, entry 4. [e] Stopped after reaction for 5 h because the reaction system became very viscous and was hard to be stirred.

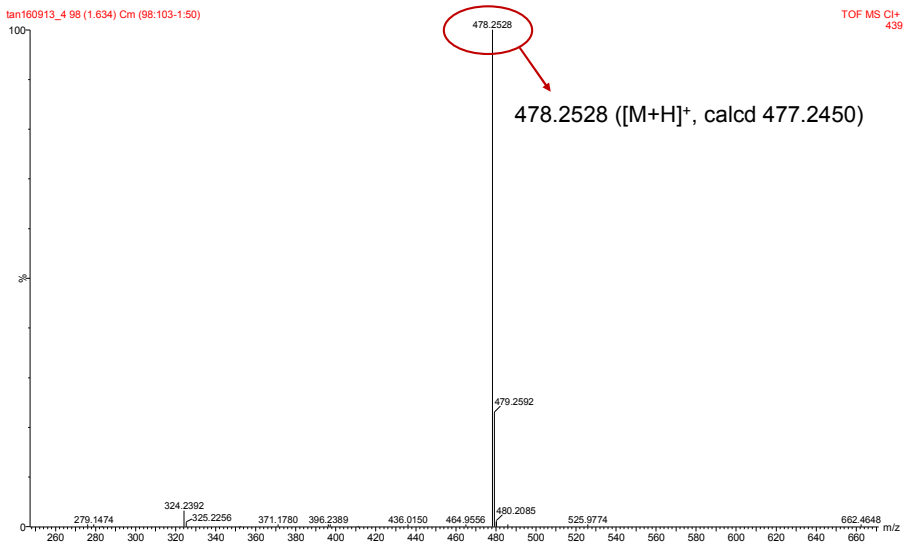

Figure S1. HRMS (CI) spectrum of **4**.

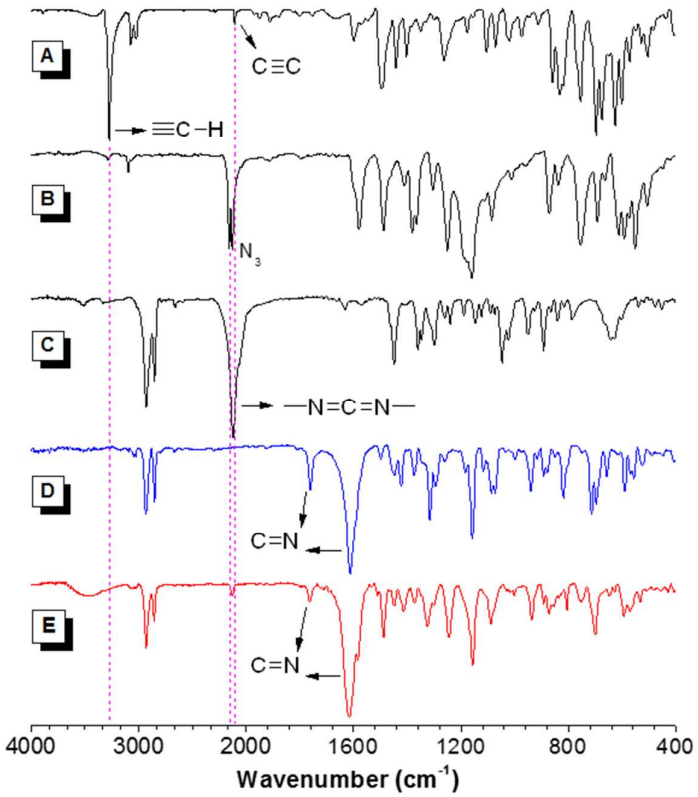

Figure S2. IR spectra of (A) **1a**, (B) **2a**, (C) **3a**, (D) **4** and (E) P**1a/2a/3a**.

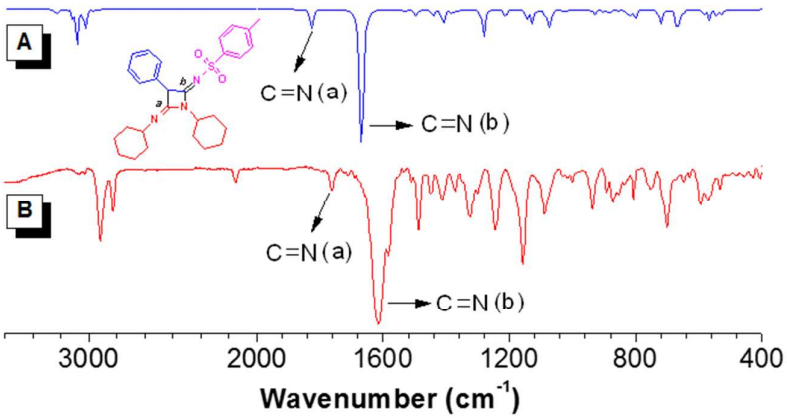

Figure S3. IR spectra of **4** obtained by (A) theoretical simulation and (B) experimental measurement. Simulation of the IR spectrum was performed by B3LYP level[4] of theory using 6-31+G** basis set for all atoms within the Gaussion 09 software package.[5]

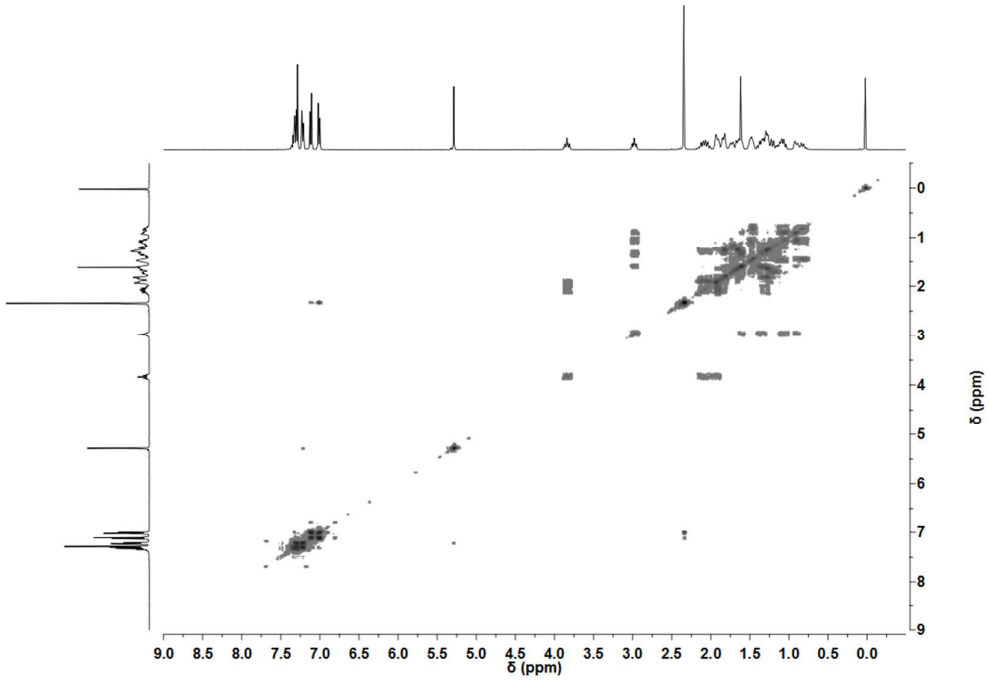

Figure S4. ^{1}H-^{1}H COSY spectrum of model compound **4** in $CDCl_3$.

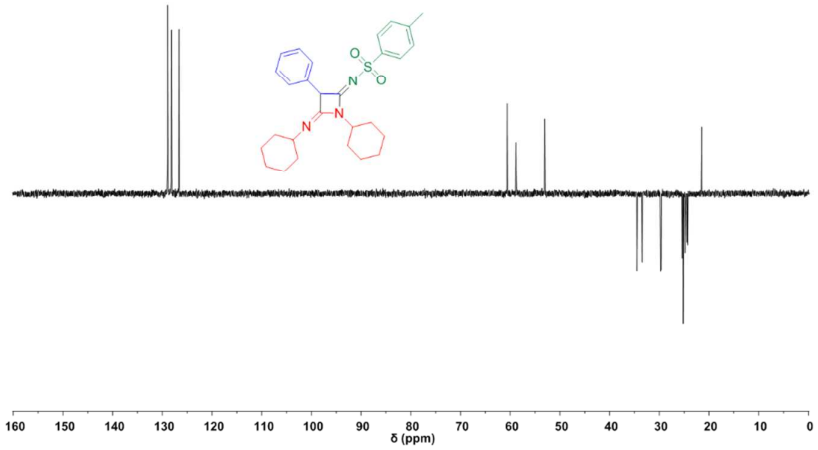

Figure S5. DEPT-135 NMR spectrum of model compound **4** in $CDCl_3$.

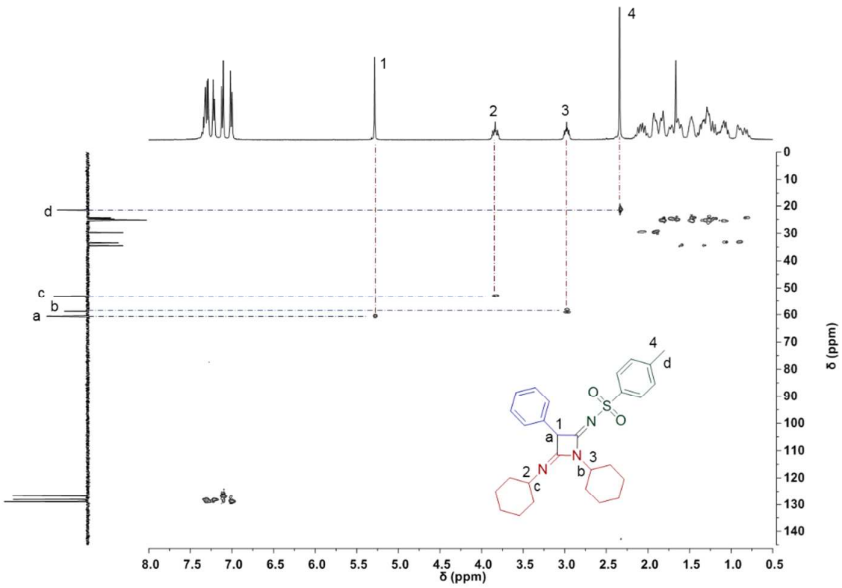

Figure S6. HSQC spectrum of model compound **4** in $CDCl_3$.

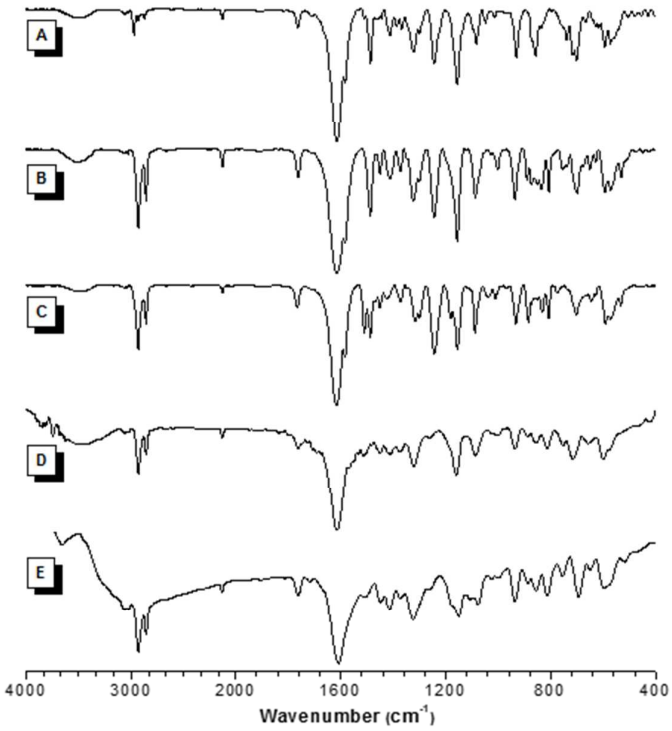

Figure S7. IR spectra of (A) P**1a/2a/3b**, (B) P**1b/2a/3a**, (C) P**1c/2a/3a**, (D) P**1a/2b/3a**, and (E) P**1a/2c/3a**.

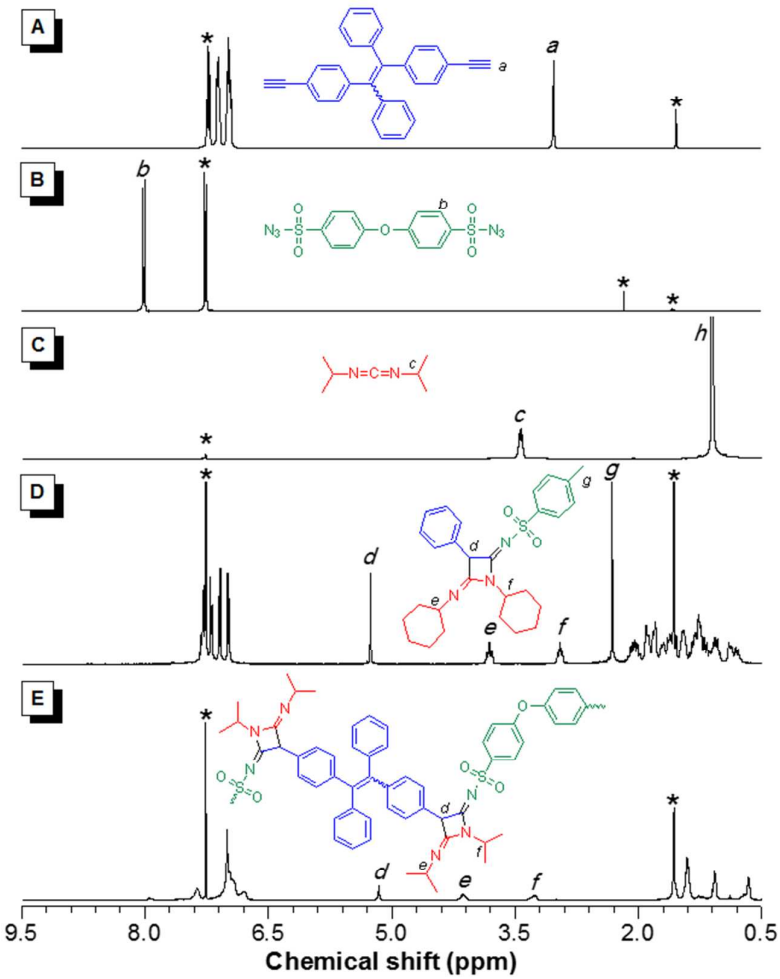

Figure S8. ^{1}H NMR spectra of (A) **1a**, (B) **2a**, (C) **3b**, (D) **4** and (E) P**1a/2a/3b** in chloroform-*d*. The solvent peaks are marked with asterisks.

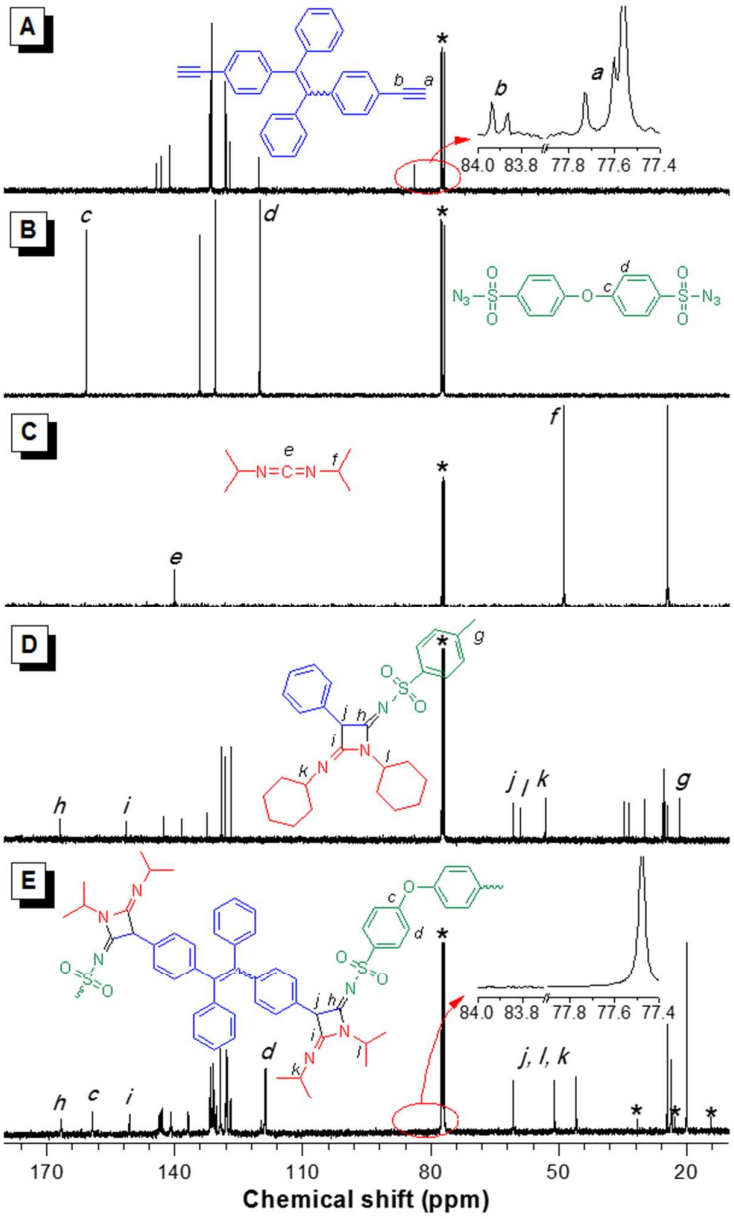

Figure S9. ^{13}C NMR spectra of (A) **1a**, (B) **2a**, (C) **3b**, (D) **4** and (E) P**1a/2a/3b** in chloroform-*d*. The solvent peaks are marked with asterisks.

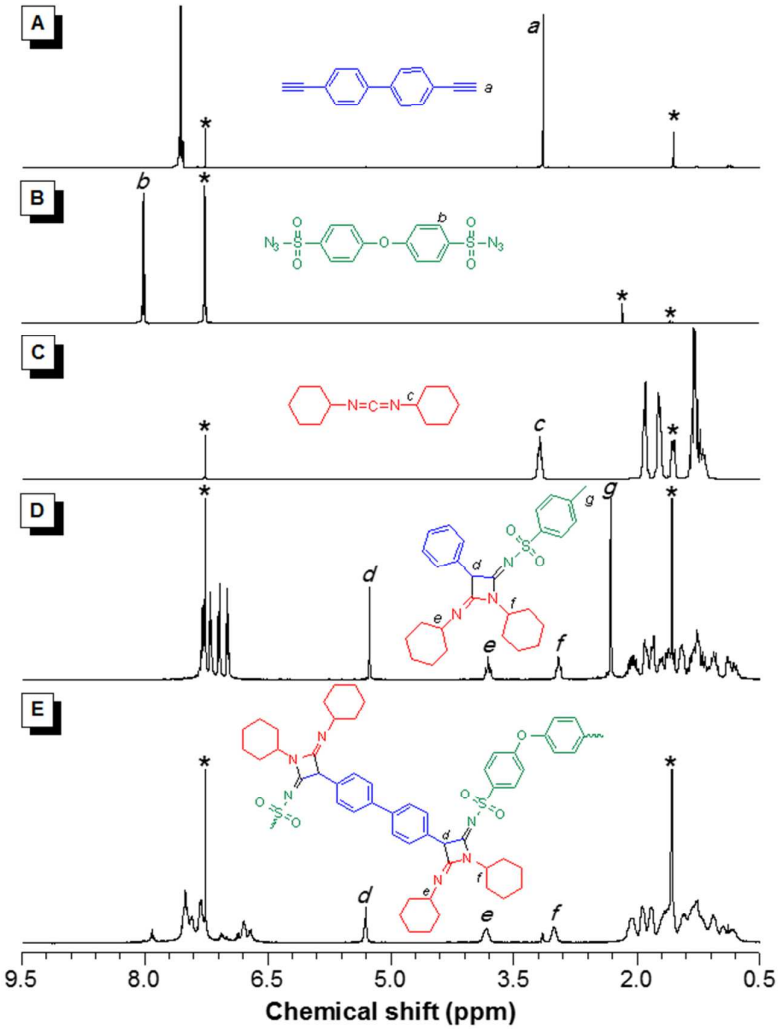

Figure S10. ^{1}H NMR spectra of (A) **1b**, (B) **2a**, (C) **3a**, (D) **4** and (E) P**1b/2a/3a** in chloroform-*d*. The solvent peaks are marked with asterisks.

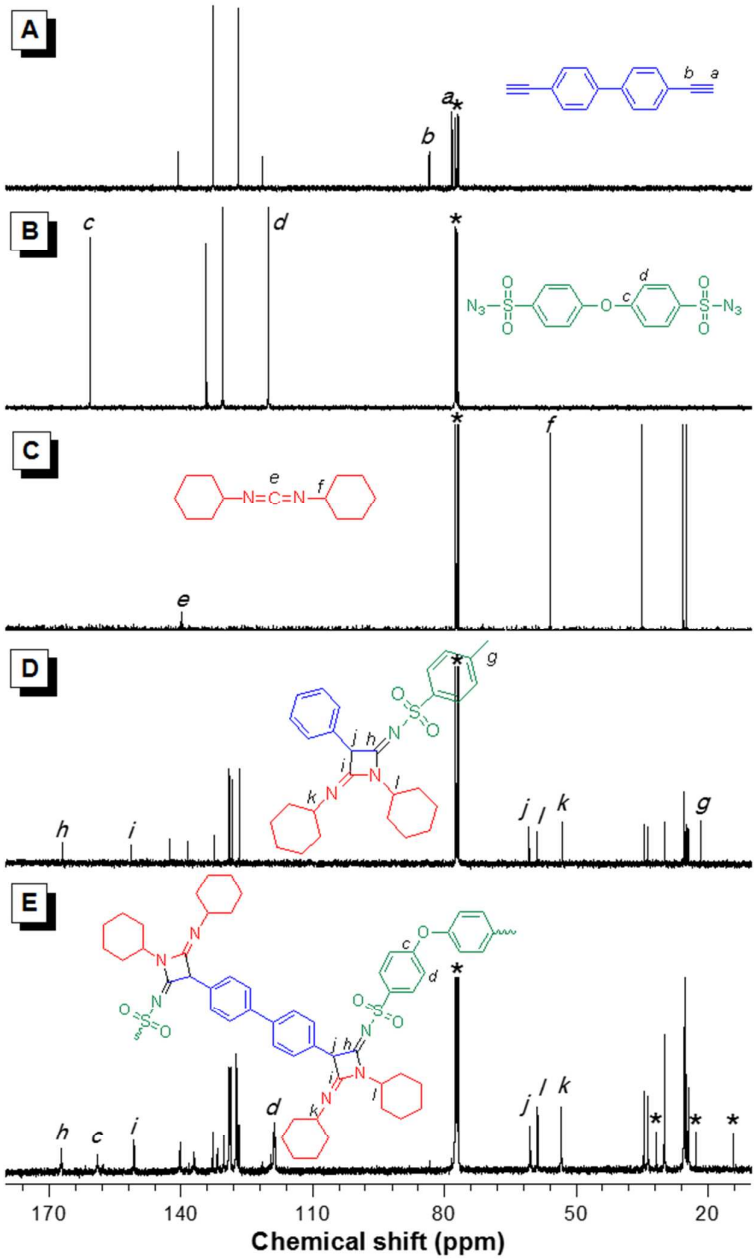

Figure S11. ^{13}C NMR spectra of (A) **1b**, (B) **2a**, (C) **3a**, (D) **4** and (E) P**1b/2a/3a** in chloroform-*d*. The solvent peaks are marked with asterisks.

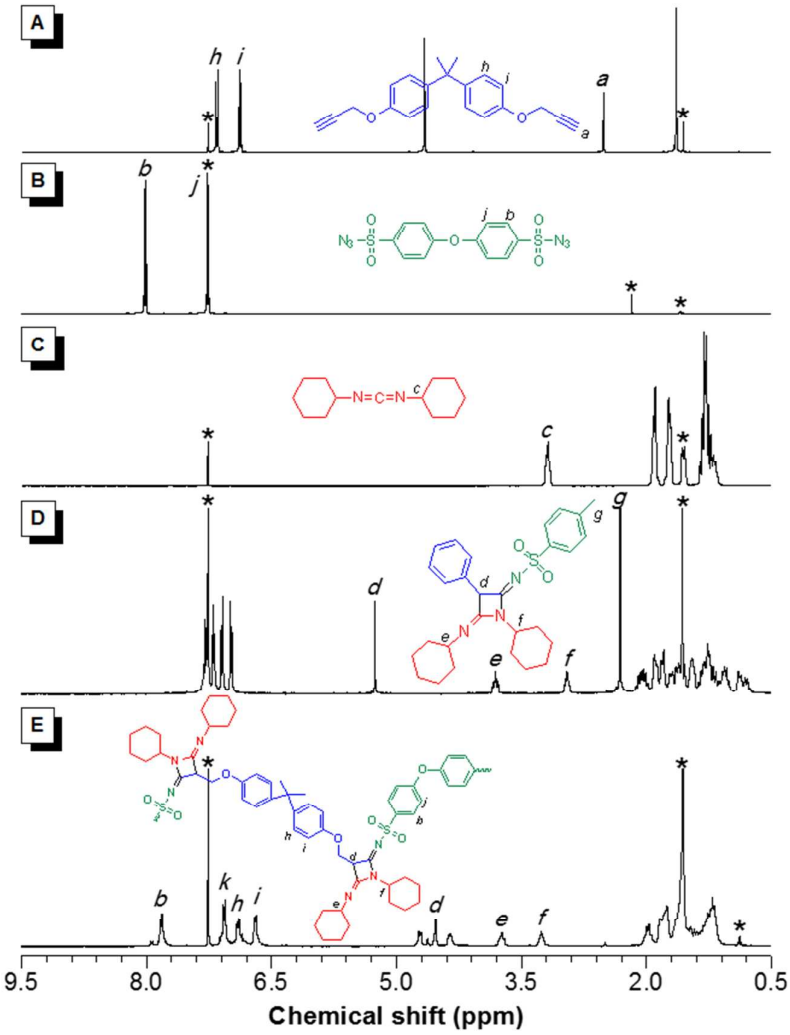

Figure S12. ^{1}H NMR spectra of (A) **1c**, (B) **2a**, (C) **3a**, (D) **4** and (E) P**1c/2a/3a** in chloroform-*d*. The solvent peaks are marked with asterisks.

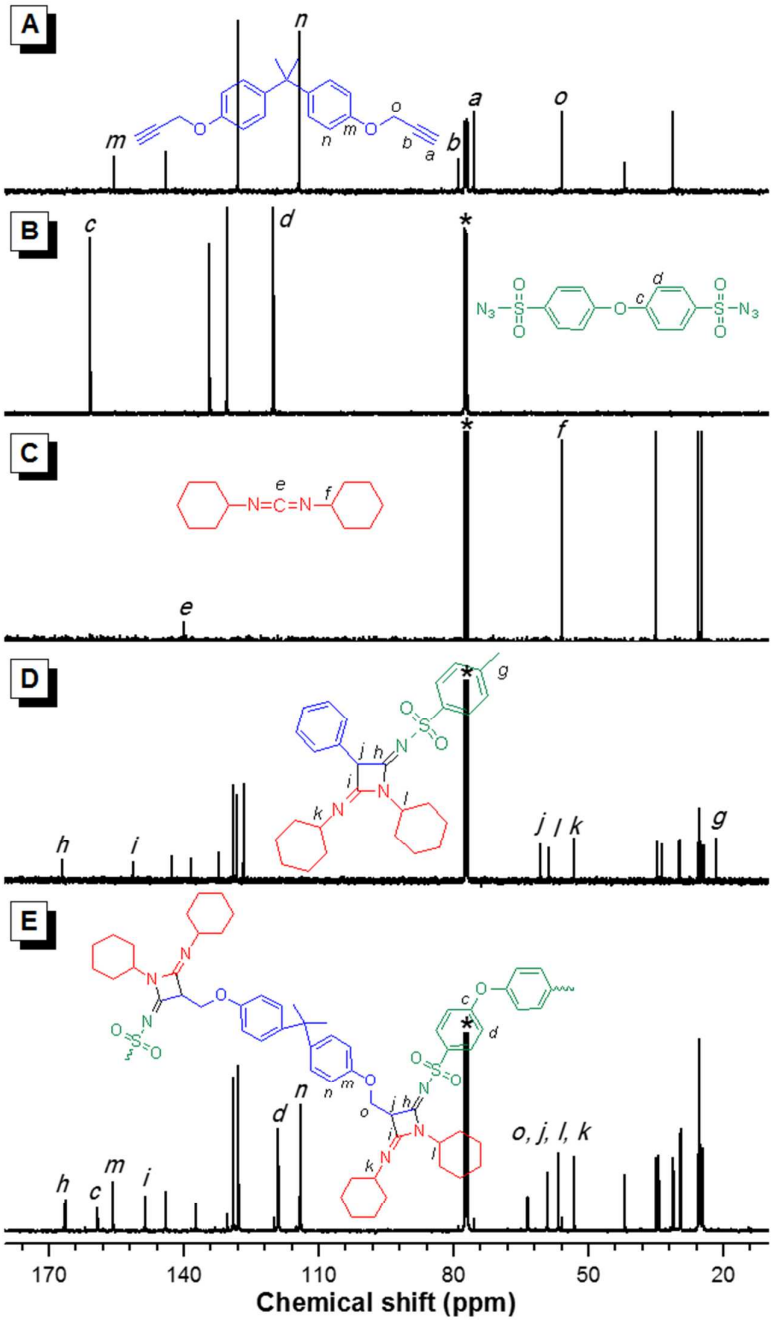

Figure S13. ^{13}C NMR spectra of (A) **1c**, (B) **2a**, (C) **3a**, (D) **4** and (E) P**1c/2a/3a** in chloroform-*d*. The solvent peaks are marked with asterisks.

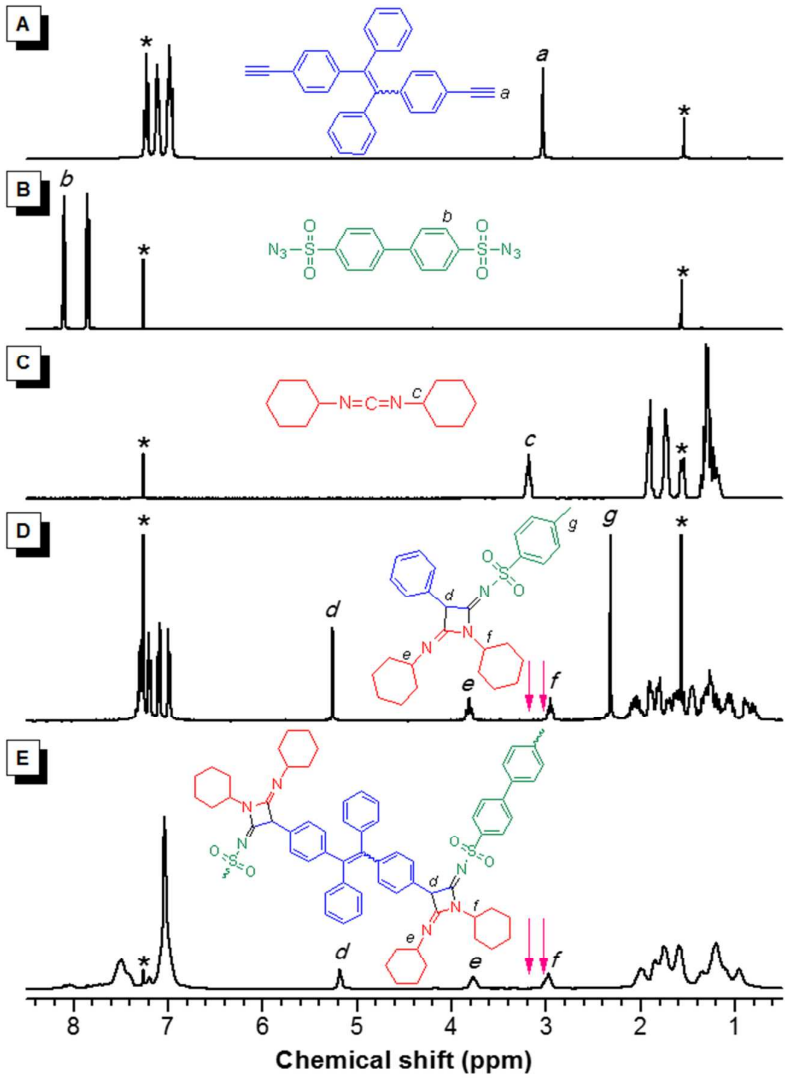

Figure S14. ^{1}H NMR spectra of (A) **1a**, (B) **2b**, (C) **3a**, (D) **4** and (E) P**1a/2b/3a** in chloroform-*d*. The solvent peaks are marked with asterisks.

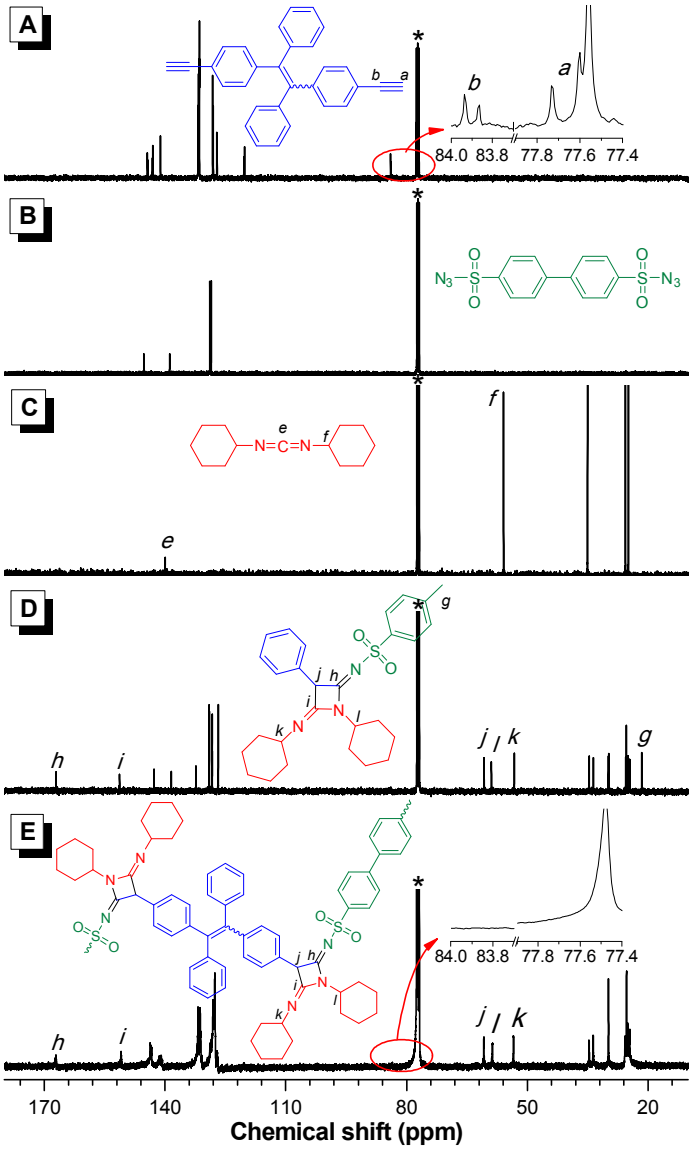

Figure S15. ^{13}C NMR spectra of (A) **1a**, (B) **2b**, (C) **3a**, (D) **4** and (E) P**1a/2b/3a** in chloroform-*d*. The solvent peaks are marked with asterisks.

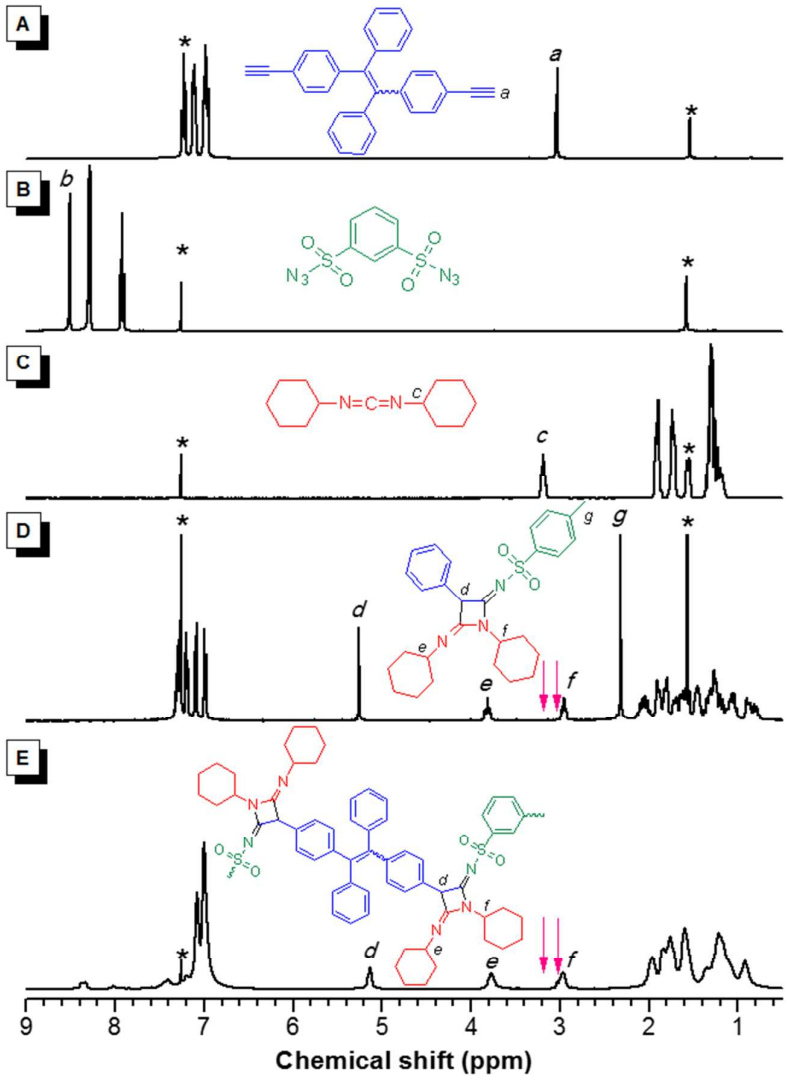

Figure S16. ^{1}H NMR spectra of (A) **1a**, (B) **2c**, (C) **3a**, (D) **4** and (E) P**1a/2c/3a** in chloroform-*d*. The solvent peaks are marked with asterisks.

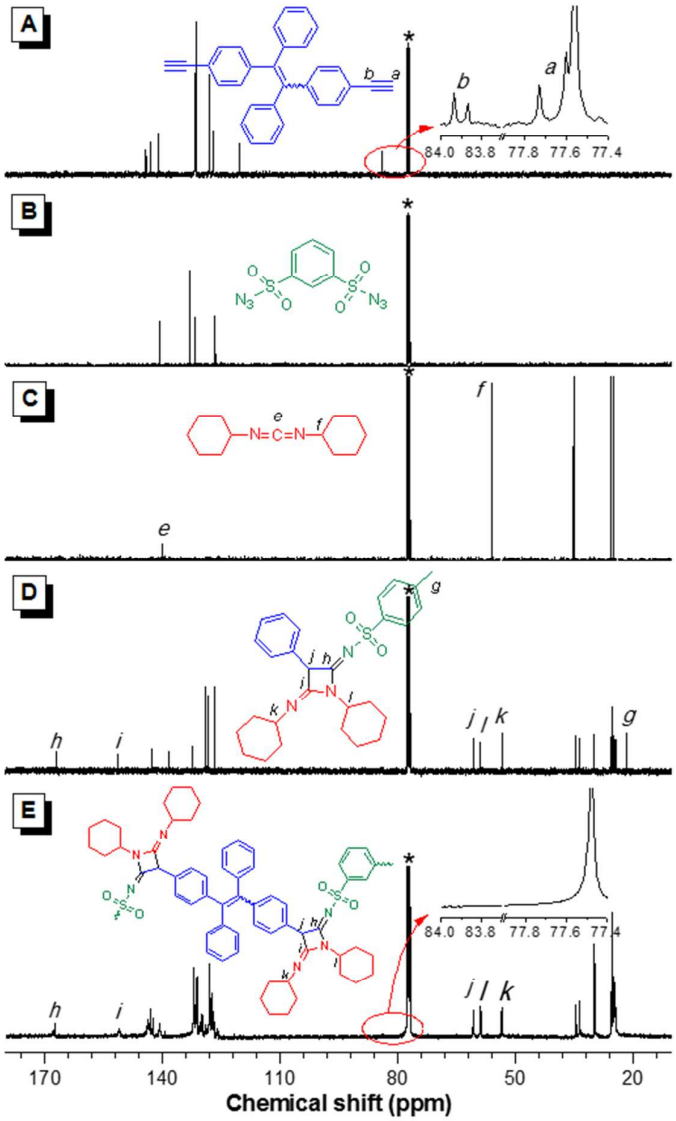

Figure S17. ^{13}C NMR spectra of (A) **1a**, (B) **2c**, (C) **3a**, (D) **4** and (E) P**1a/2c/3a** in chloroform-*d*. The solvent peaks are marked with asterisks.

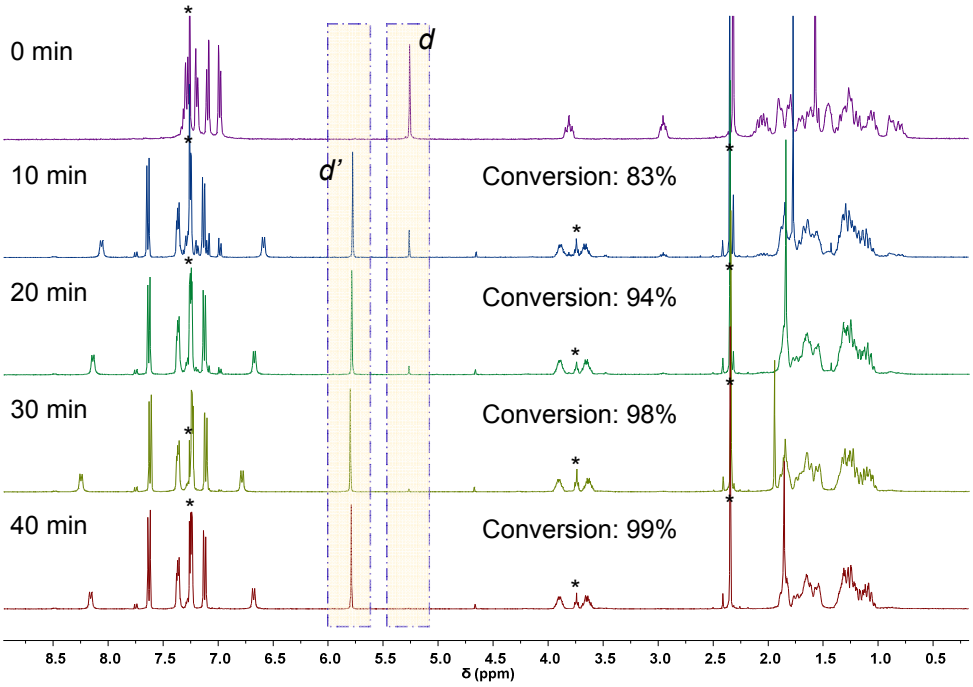

Figure S18. ^{1}H NMR spectra of the model compound in chloroform-*d* before and after ring-opening reaction for different time. The solvent peaks are marked with asterisks.

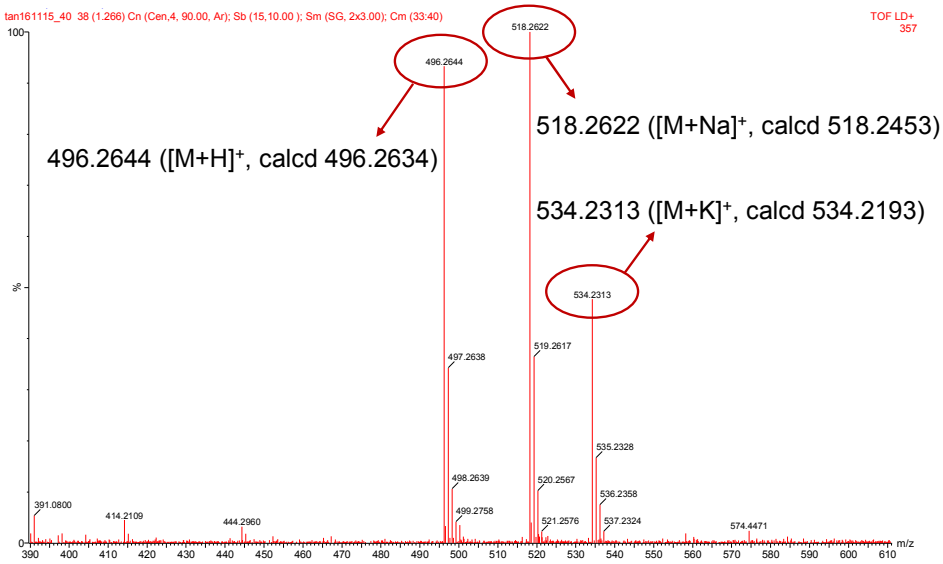

Figure S19. HRMS (MALDI-TOF) spectrum of **5**.

Table S5. Crystal Data and Structure Refinement of Model Compound 5

Crystal data	
Chemical formula	$C_{28}H_{37}N_3O_3S$
M_r	495.66
Crystal system, space group	Monoclinic, $P2_1/c$
Temperature (K)	150
a, b, c (Å)	9.706 (2), 25.862 (7), 11.622 (3)
β (°)	114.351 (3)
V (Å^3)	2657.8 (11)
Z	4
Radiation type	Mo $K\alpha$
μ (mm^{-1})	0.16
Crystal size (mm^3)	0.53 × 0.41 × 0.12
Data collection	
Diffractometer	Bruker *APEX* 2 CCD area detector diffractometer
Absorption correction	Multi-scan *SADABS* v2014/5, Sheldrick, G.M., (2014)
T_{min}, T_{max}	0.922, 0.982
No. of measured, independent and observed [$I > 2\sigma(I)$] reflections	17313, 5429, 3283
R_{int}	0.075
$(\sin \theta/\lambda)_{max}$ (Å^{-1})	0.626
Refinement	
$R[F^2 > 2\sigma(F^2)]$, $wR(F^2)$, S	0.055, 0.132, 1.01

No. of reflections	5429
No. of parameters	371
No. of restraints	153
H-atom treatment	H atoms treated by a mixture of independent and constrained refinement
$\Delta\rangle_{max}$, $\Delta\rangle_{min}$ (e Å^{-3})	0.29, -0.34

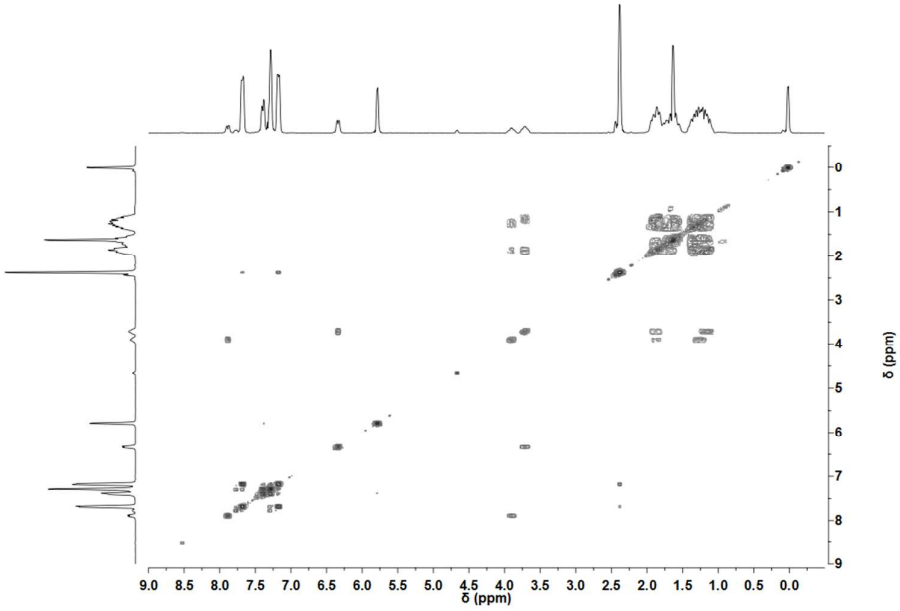

Figure S20. ^{1}H-^{1}H COSY spectrum of model compound **5** in $CDCl_3$.

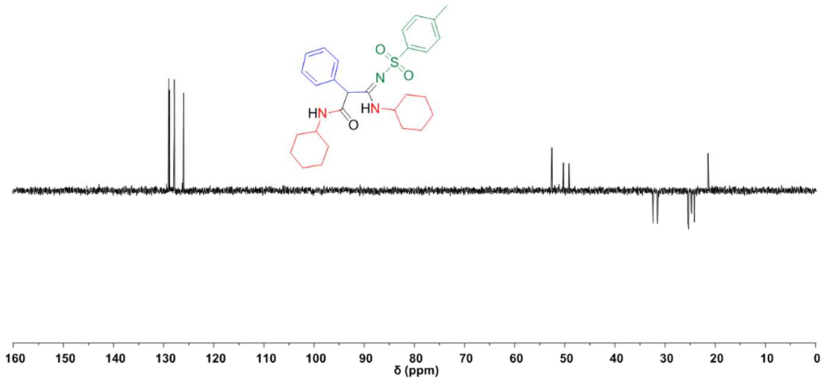

Figure S21. DEPT-135 NMR spectrum of model compound **5** in $CDCl_3$.

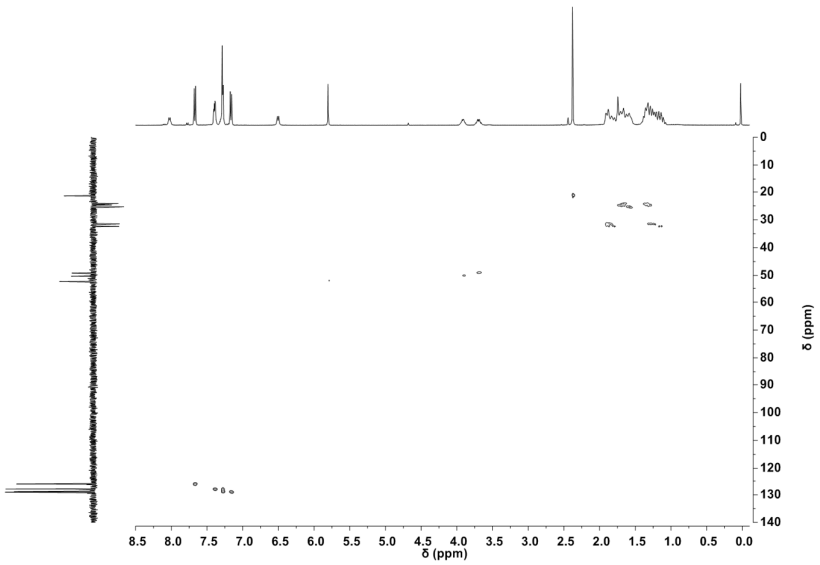

Figure S22. HSQC spectrum of model compound **5** in $CDCl_3$.

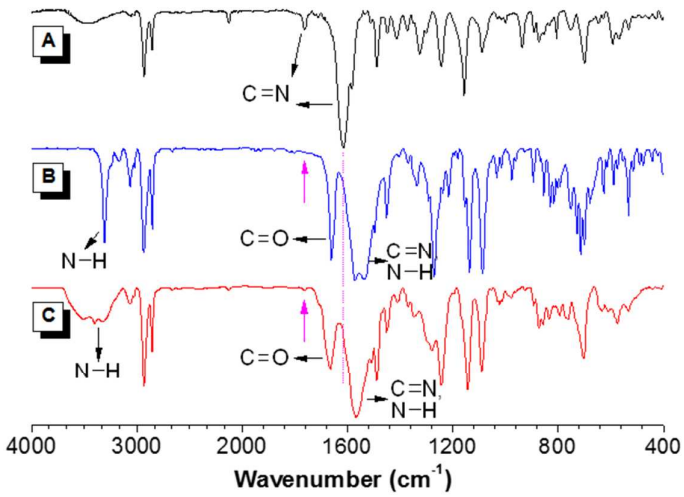

Figure S23. IR spectra of (A) P**1a/2/3a**, (B) **5** and (C) P**5** (sample obtained from the ring-opening reaction for 30 min).

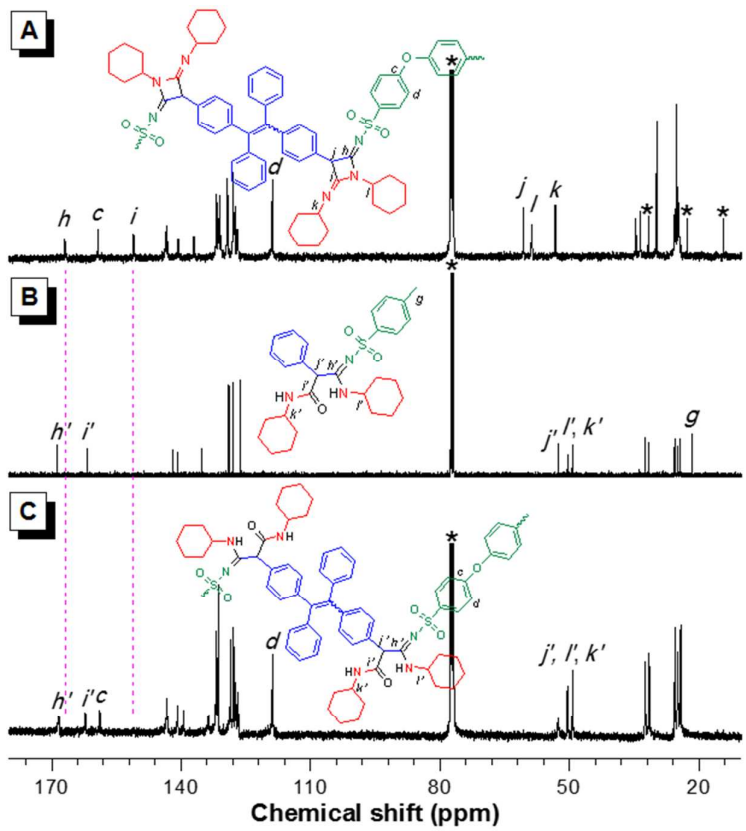

Figure S24. ^{13}C NMR spectra of (A) P**1a/2/3a**, (B) **5** and (C) P**5** (sample obtained from the ring-opening reaction for 30 min) in chloroform-*d*. The solvent peaks are marked with asterisks.

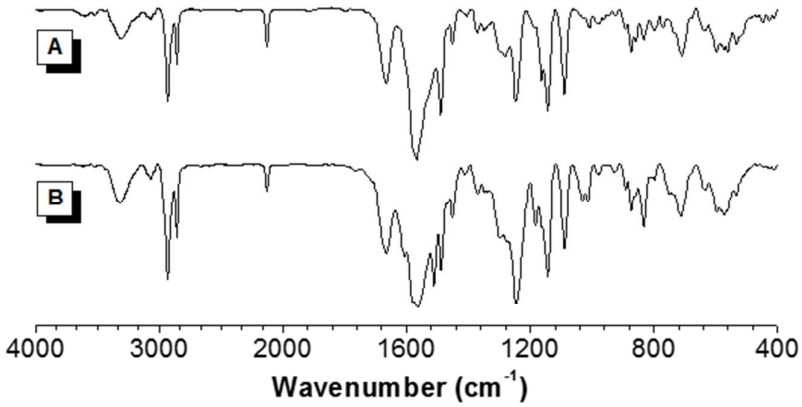

Figure S25. IR spectra of (A) P**6** and (B) P**7**.

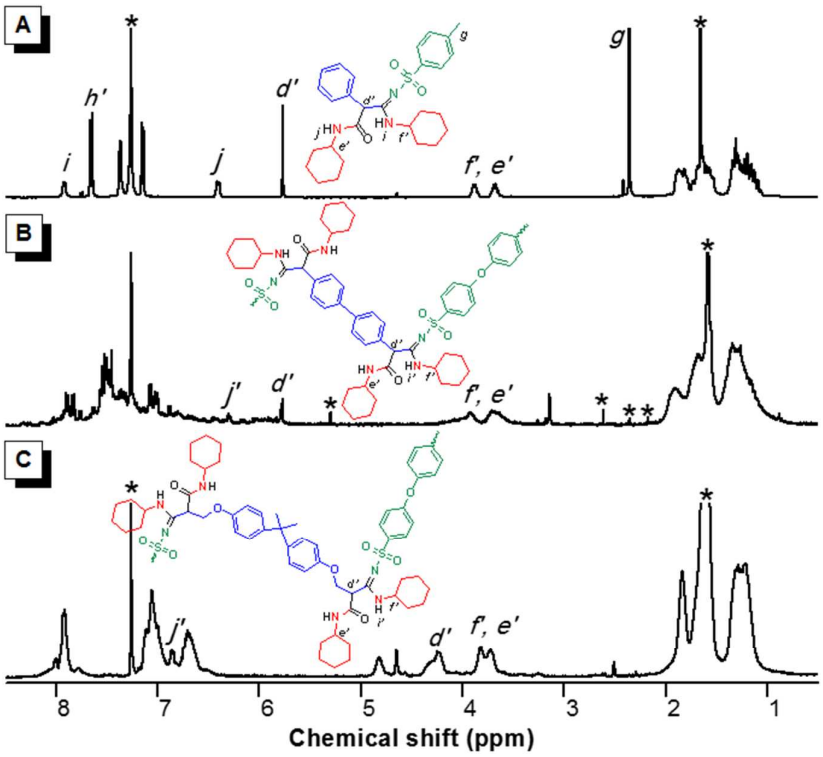

Figure S26. ^{1}H NMR spectra of (A) **5**, (B) P**6** and (C) P**7** in chloroform-*d*. The solvent peaks are marked with asterisks.

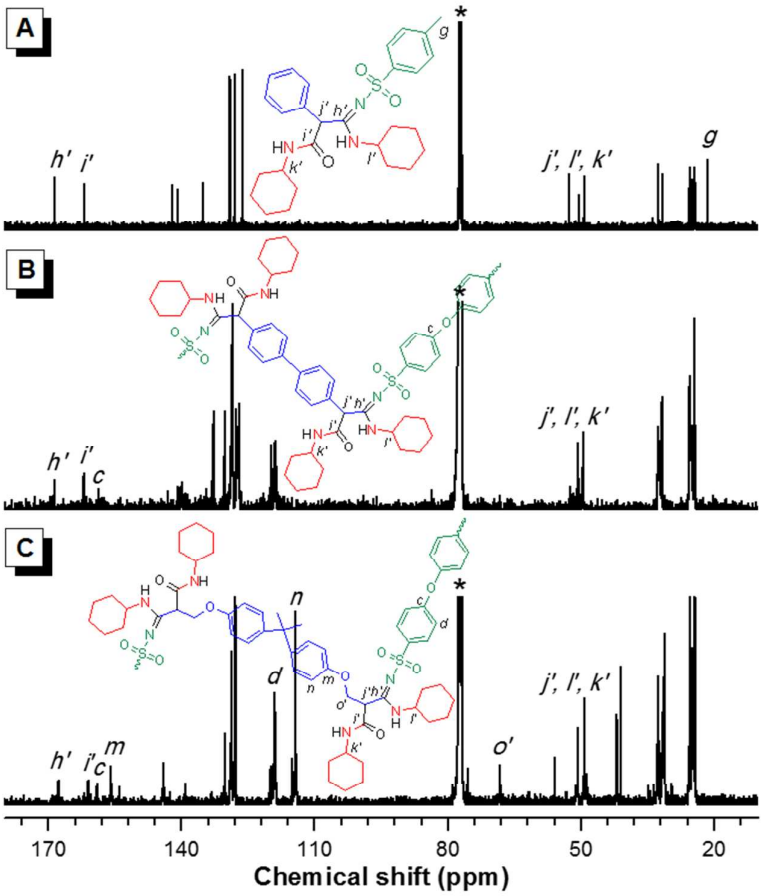

Figure S27. ^{13}C NMR spectra of (A) **5**, (B) P**6** and (C) P**7** in chloroform-*d*. The solvent peaks are marked with asterisks.

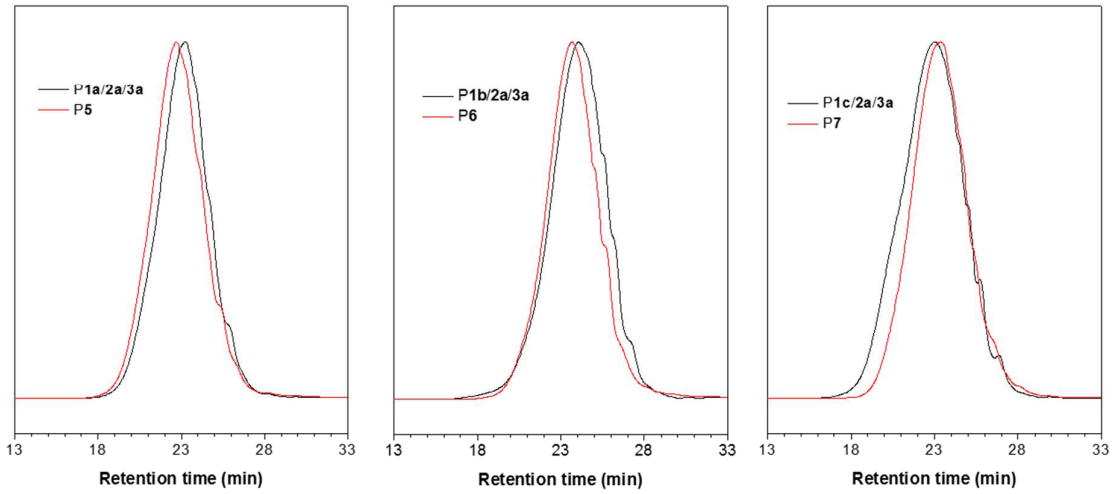

Figure S28. GPC curves of polymers before and after ring-opening reaction.

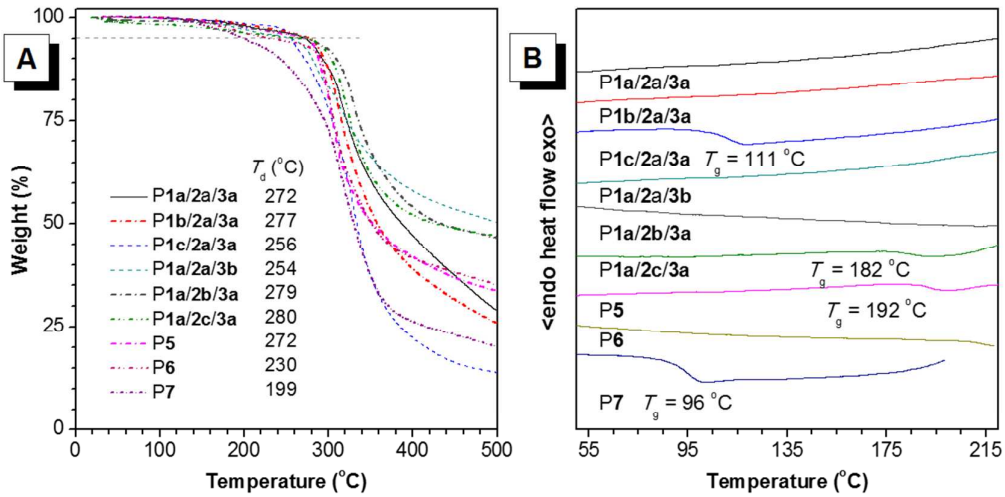

Figure S29. (A) TGA thermograms of P**1a–c/2a–c/3a–b** and P**5–7** recorded under nitrogen at a heating rate of 10 °C/min. (B) DSC thermograms of P**1a–c/2a–c/3a–b** and P**5–7** recorded under nitrogen during the second heating cycle at a heating rate of 10 °C/min.

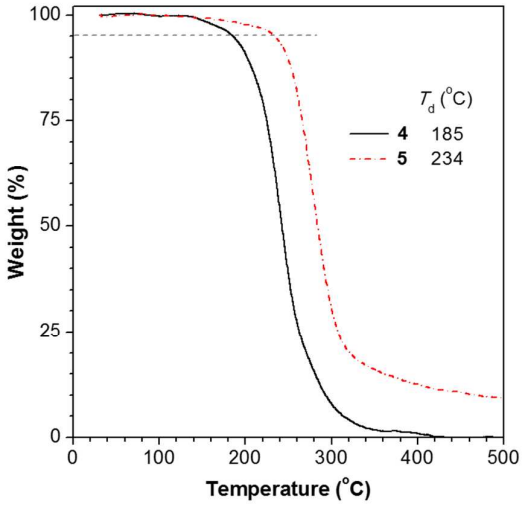

Figure S30. TGA thermograms of model compounds **4** and **5** recorded under nitrogen at a heating rate of 10 °C/min.

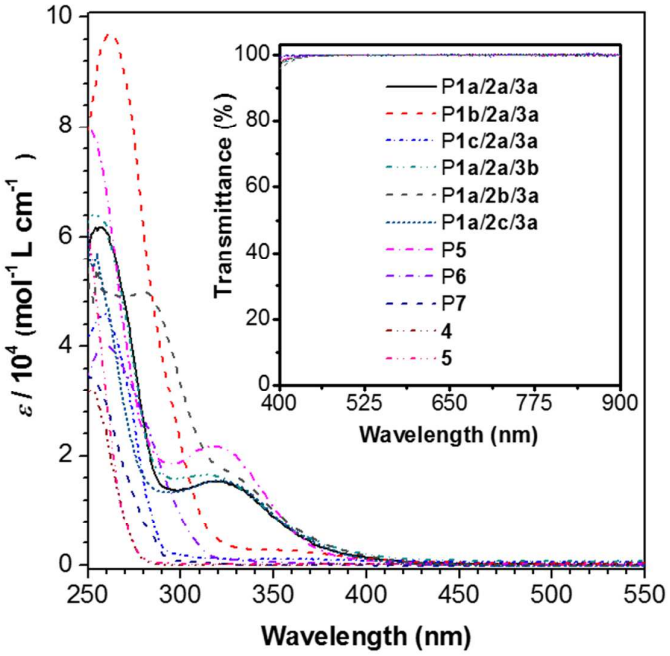

Figure S31. UV spectra of P**1a–c/2a–c/3a–b**, P**5–7**, **4** and **5** in THF solutions. Solution concentration: 10 μM. Inset: transmission spectra of P**1a–c/2a–c/3a–b** and P**5–7** in THF solutions at wavelengths from 400 to 900 nm.

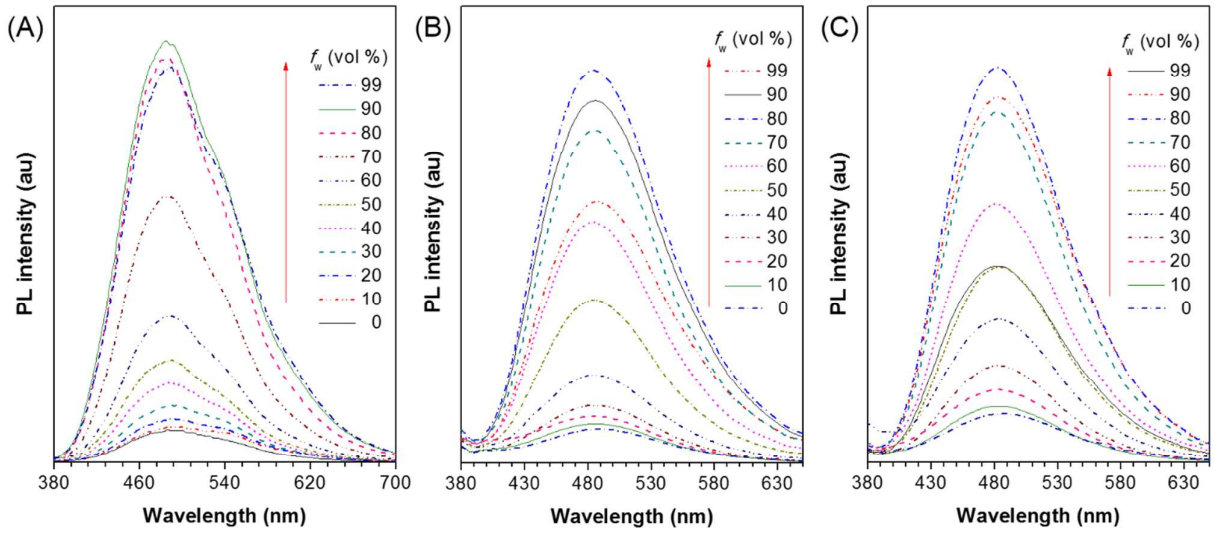

Figure S32. PL spectra of (A) P**1a/2a/3b**, (B) P**1a/2b/3a** and (C) P**1a/2c/3a** in THF and THF/water mixtures with different water fractions (f_w). Solution concentration: 10 μM; excitation wavelength: 320 nm.

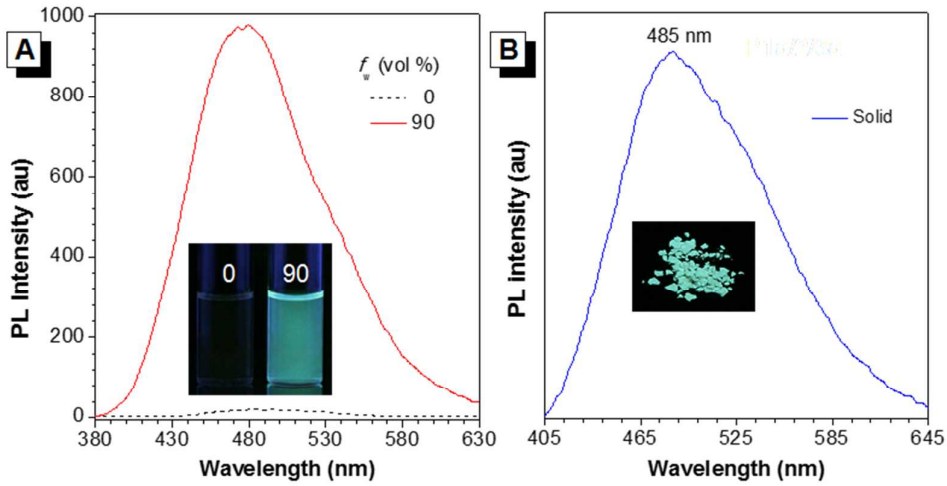

Figure S33. (A) PL spectra of P**5** in THF and THF/water mixture with 90% water fraction (f_w). Inset: fluorescent photographs of P**5** in THF/water mixtures with f_w of 0% and 90% taken under 365 nm UV irradiation. Solution concentration: 10 μM; excitation wavelength: 320 nm. (B) PL spectra of P**5** in solid state and the associated fluorescent photos taken under 365 nm UV irradiation. Excitation wavelength: 320 nm.

Table S6. Optical properties of P**1a/2a/3a and** P**5**[a]

polymer	$\lambda_{em,soln}$	$\lambda_{em,aggr}$	I_{90}/I_0	Φ_{soln}	Φ_{aggr}	Φ_{powder}	α_{AIE}
P**1a/2a/3a**	489	484	17	1.4%	8.2%	11.2%	8
P**5**	487	483	48	1.4%	11.5%	27.1%	19

[a] Abbreviation: $\lambda_{em,soln}$ and $\lambda_{em,aggr}$ = wavelength of the emission maximum in THF solution and aggregate state, respectively; I_{90} and I_0 represents the PL intensity at f_w = 90% and 0%, respectively; $\alpha_{AIE} = \Phi_{aggr}/\Phi_{soln}$, where Φ_{soln}, Φ_{aggr}, Φ_{powder} = the fluorescent quantum yield of the THF solution, aggregates in THF/water mixture with f_w of 90%, and the solid powder of the polymers, respectively.

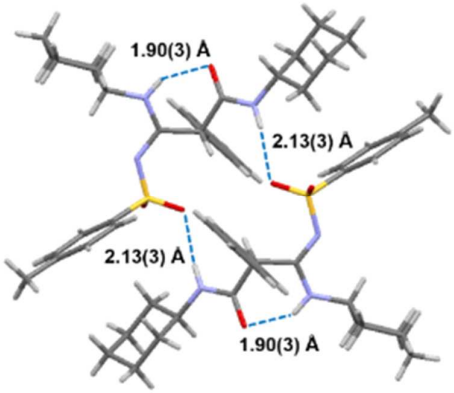

Figure S34. Illustration of H-bonding interactions in single crystals of **5**.

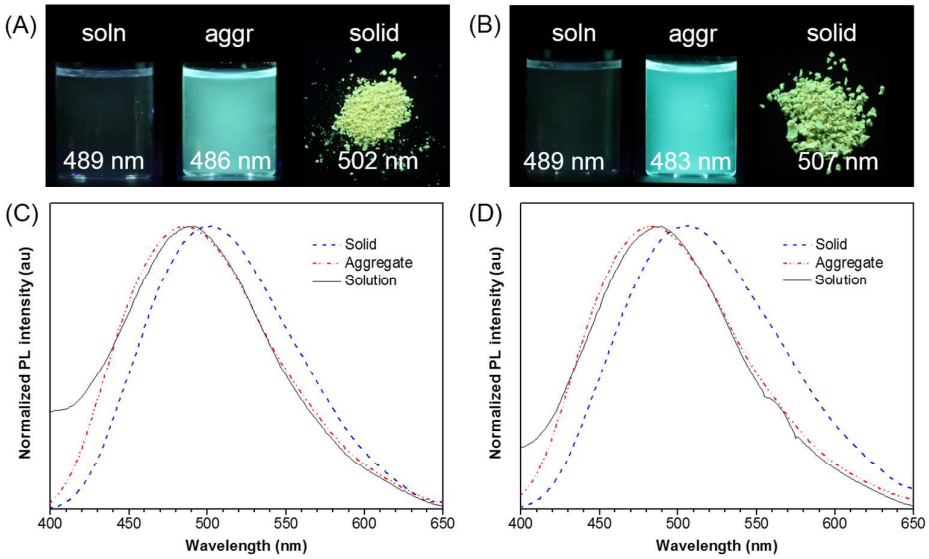

Figure S35. The normalized PL spectra of (A) P**1a**/**2b**/**3a** and (B) P**1a**/**2c**/**3a**. Inset: fluorescent photographs of (C) P**1a**/**2b**/**3a** and (D) P**1a**/**2c**/**3a** in THF solution, THF/water mixture with 90% water fraction, and solid state taken under 365 nm UV irradiation. Solution concentration: 10 μM; excitation wavelength: 320 nm.

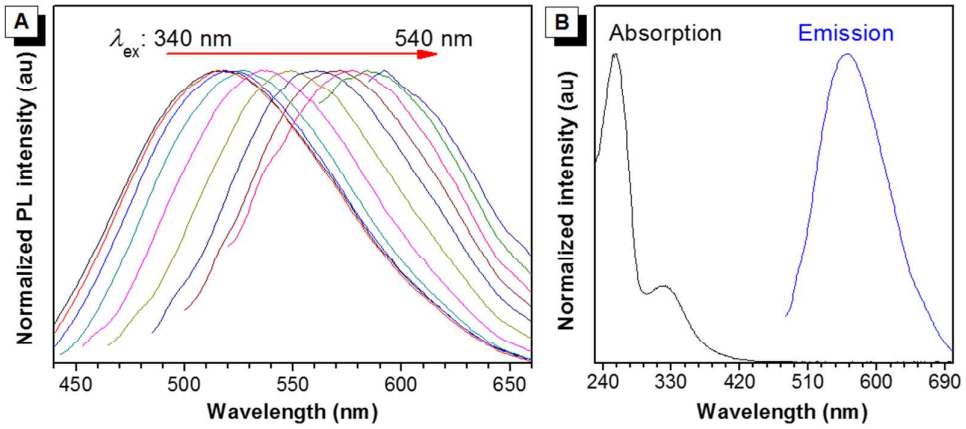

Figure S36. (A) Normalized emission spectra of P**1a/2a/3a** in the solid state at different excitation wavelengths (from 360 to 540 nm) at an interval of 20 nm. (B) Absorption spectrum of P1a/2a/3a and emission spectrum (excited at 460 nm) of P**1a/2a/3a** in the solid state.

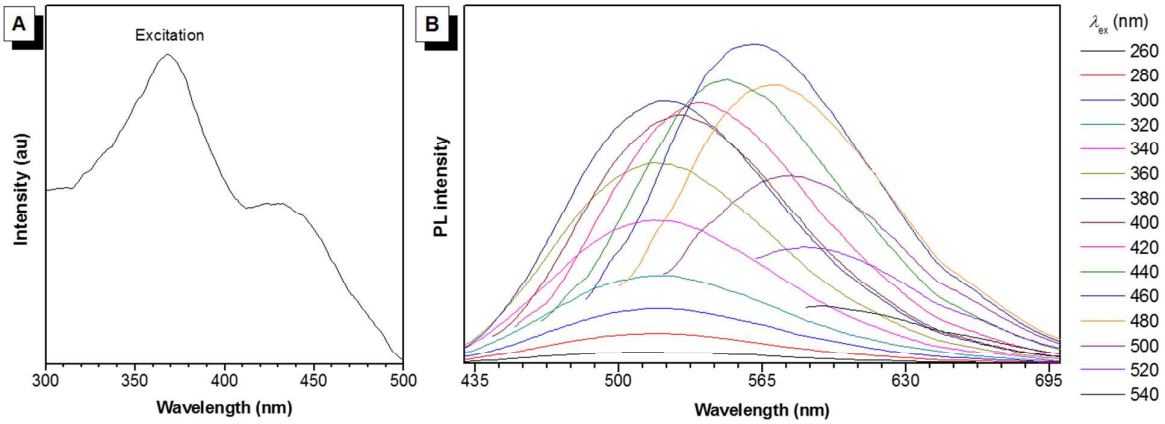

Figure S37. (A) Excitation spectrum of P**1a/2a/3a** in the solid state. (B) Fluorescence spectra of P**1a/2a/3a** in the solid state at different excitation wavelengths. The curves were fitted to hide the double frequency scattering peaks.

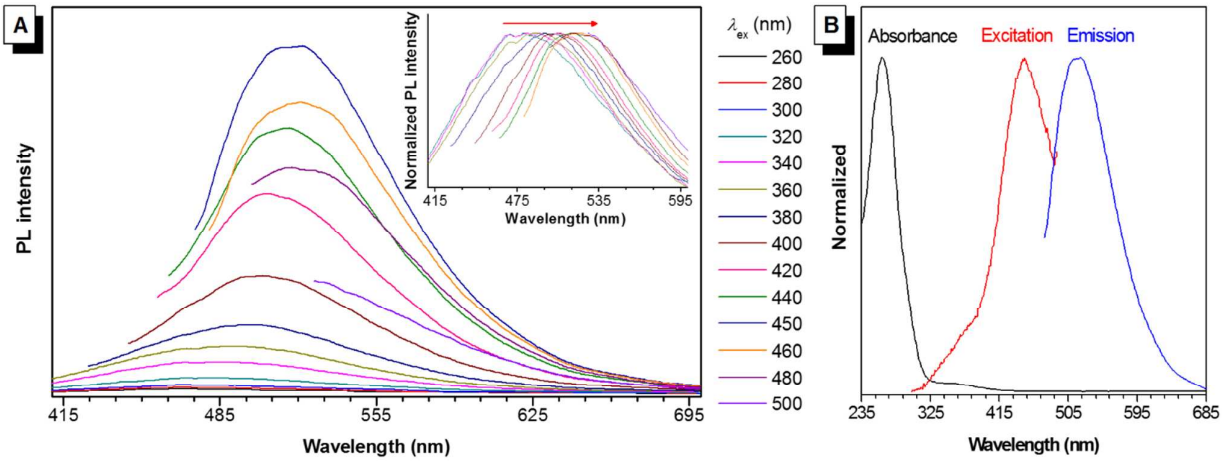

Figure S38. (A) Fluorescence spectra of P**1b/2a/3a** in the solid state at different excitation wavelengths. Inset: normalized emission spectra at excitation wavelengths from 320 to 500 nm with 20 nm increment. The curves were fitted to hide the double frequency scattering peaks. (B) Absorption spectrum of P**1b/2a/3a** in THF solution and its excitation and emission spectra (excited at 450 nm) in the solid state.

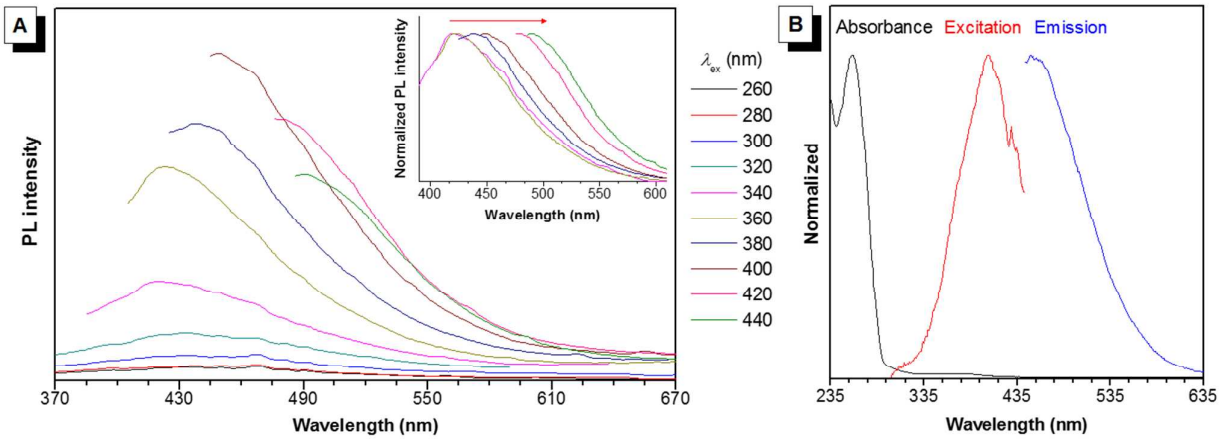

Figure S39. (A) Fluorescence spectra of P**1c/2a/3a** in the solid state at different excitation wavelengths. Inset: normalized emission spectra at excitation wavelengths ranging from 340 to 440 nm with 20 nm increment. The curves were fitted to hide the double frequency scattering peaks. (B) Absorption spectrum of P**1c/2a/3a** in THF solution and its excitation and emission spectra (excited at 400 nm) in the solid state.

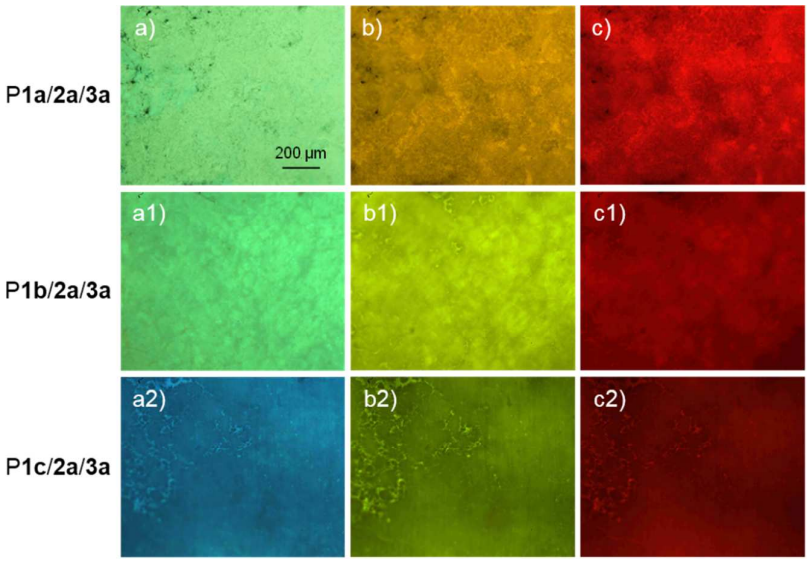

Figure S40. Fluorescent images of the polymer powders taken under a fluorescent microscope at different light illuminations. Excitation wavelength: (a–a2) 330–380 nm, (b–b2) 450–490 nm and (c–c2) 510–560 nm.

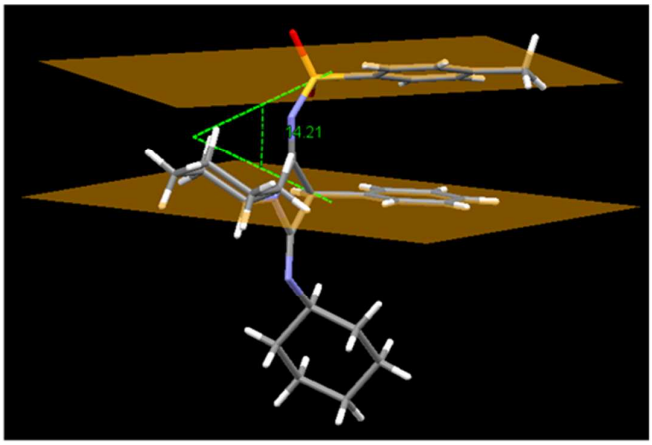

Figure S41. Tilted angle of two cofacial stacked phenyl rings in the single crystal of model compound **4**. Angles were expressed in the unit of °.

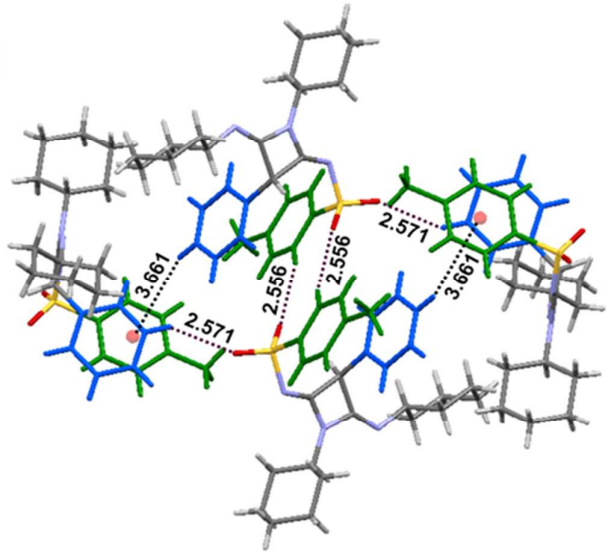

Figure S42. Illustration of intermolecular C-H···O and C-H···π interactions in single crystals of **4**. Distances were expressed in the unit of Å.

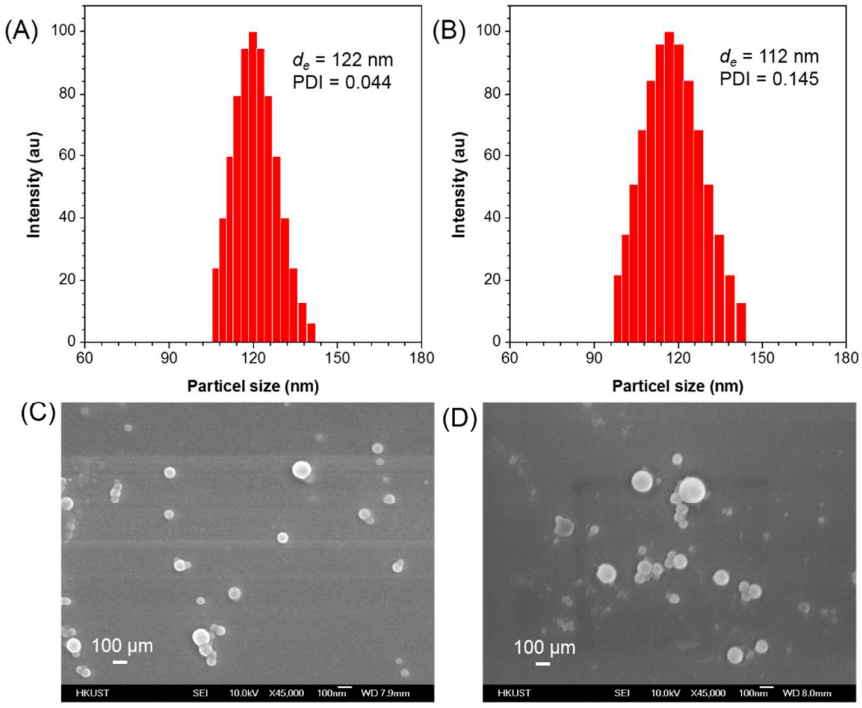

Figure S43. Particle size distributions of the nanoparticles of (A) P**1a/2a/3a** and (B) P**5** measured by dynamic light scattering. Abbreviation: d_e = effective diameter, PDI = polydispersity index. SEM images of nanoparticles of (C) P**1a/2a/3a** and (D) P**5**.

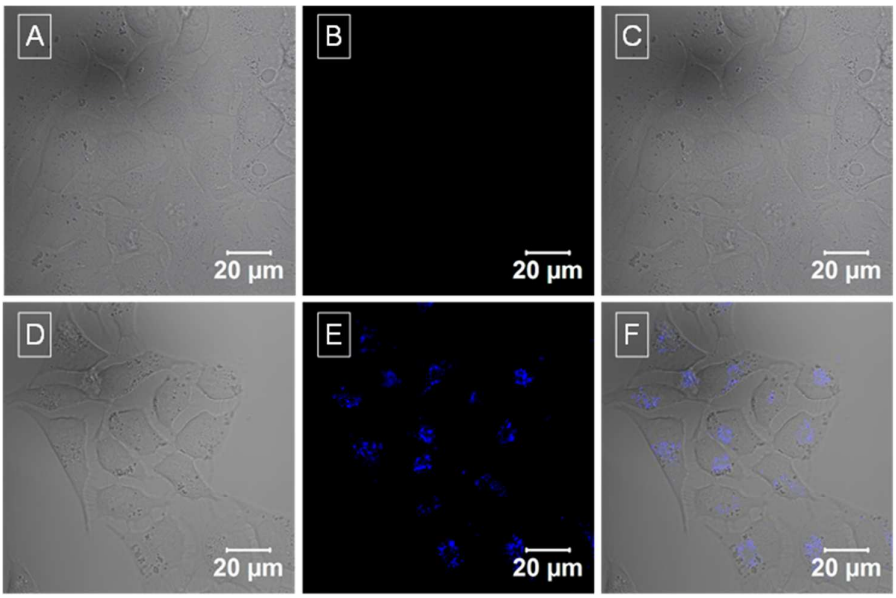

Figure S44. (A and D) Bright field image, (B and E) fluorescent image, and (C and F) the associated merged image of HeLa cells stained with 120 μg/mL of P**1a**/**2a**/**3a** (upper panel) and P**5** (lower panel) nanoparticles for 18 h. Excitation wavelength: 405 nm; emission filter: 410–740 nm (for P**1a**/**2a**/**3a**) and 410–509 nm (for P**5**).

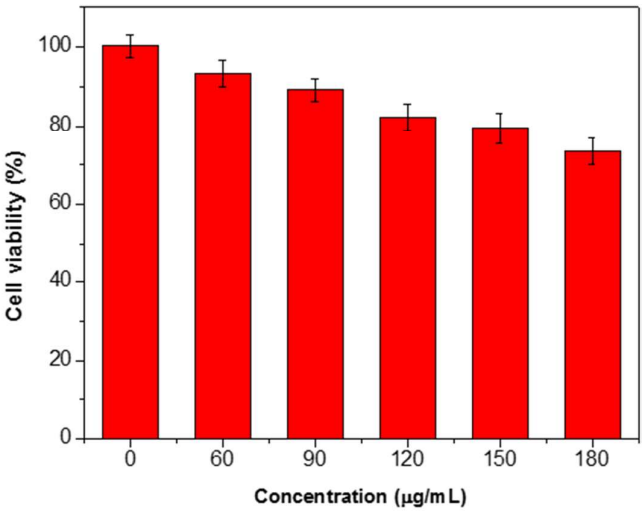

Figure S45. Cell viability of HeLa cells in the presence of P**5** nanoparticles at different concentrations.

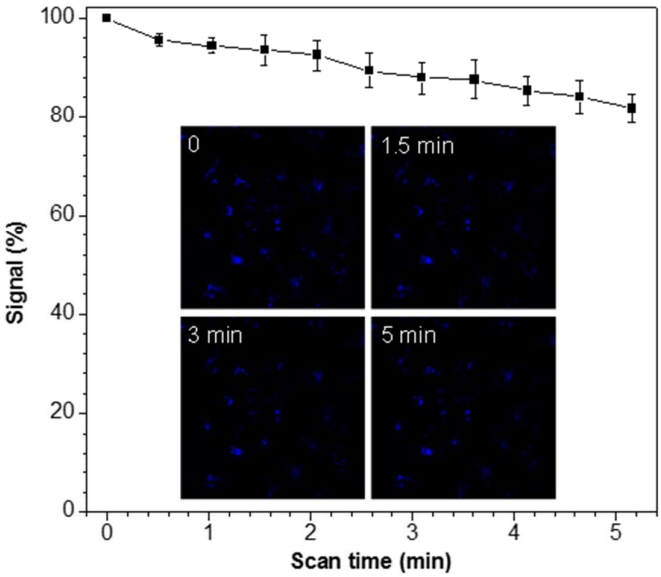

Figure S46. Change in fluorescent signal from HeLa cells stained with P**5** nanoparticles (120 μg/mL) with the scan time. Excitation wavelength: 405 nm; laser power: 2%. Inset: fluorescence images of HeLa cells obtained at different irradiation time.

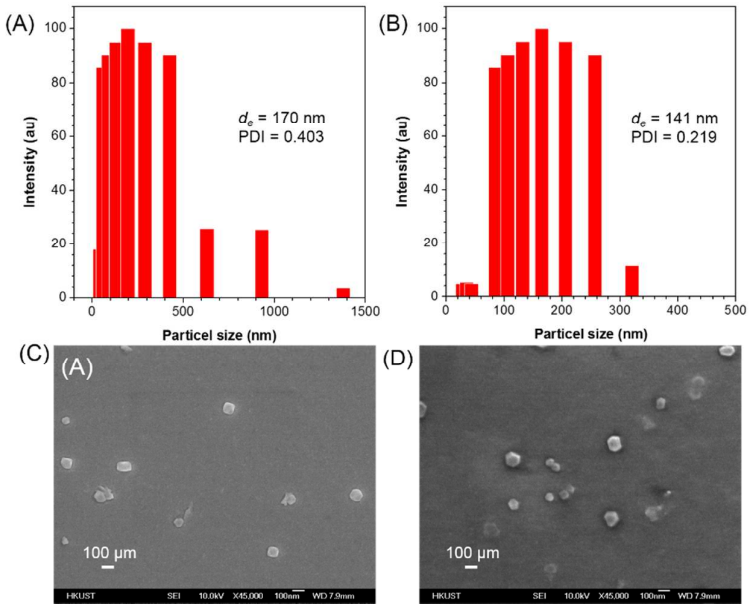

Figure S47. Particle size distributions of the nanoparticles of (A) **4** and (B) **5** measured by dynamic light scattering. Abbreviation: d_e = effective diameter, PDI = polydispersity. SEM images of nanoparticles of (C) **4** and (D) **5**.

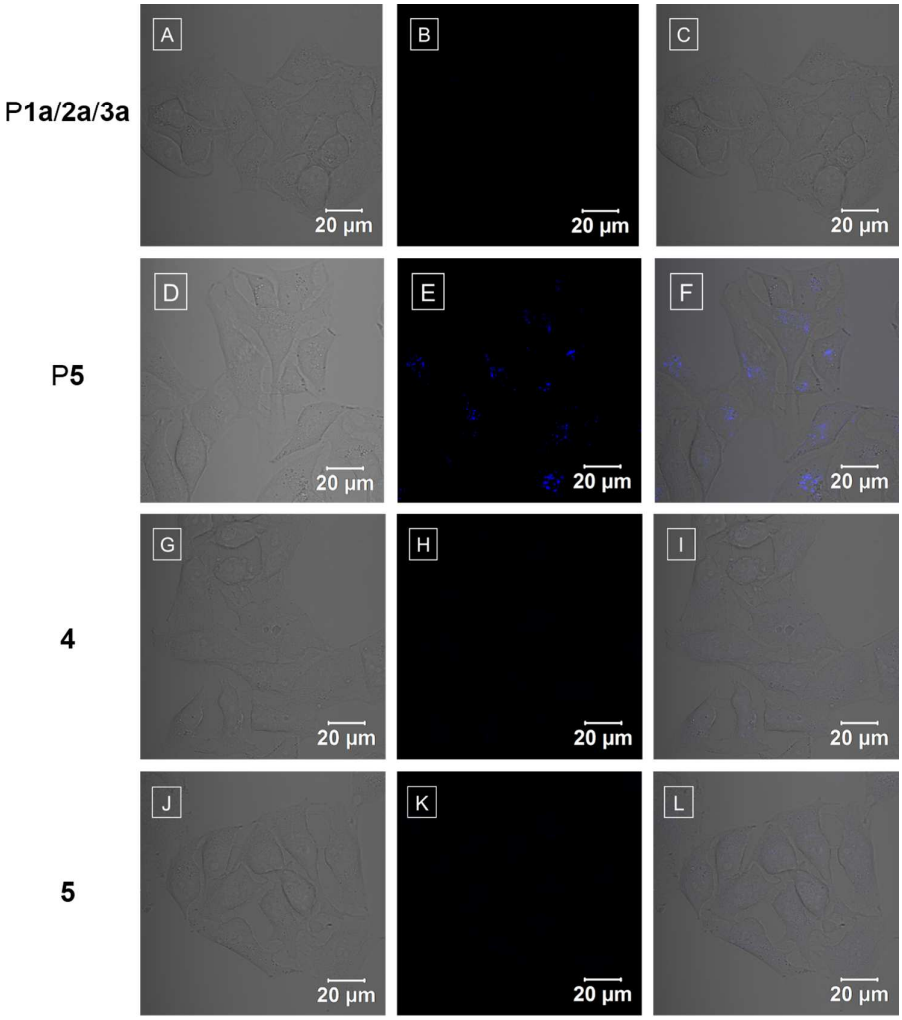

Figure S48. (A, D, G, and J) Bright-field images, (B, E, H, and K) fluorescent images, and (C, F, I, and L) the associated merged images of HeLa cells stained with 120 μg/mL of nanoparticles of P**1a/2a/3a**, P**5**, **4**, and **5** for 18 h. Excitation wavelength: 405 nm; emission filter: 410–740 nm (for P**1a/2a/3a**) and 410–509 nm (for P**5**, **4** and **5**).

Table S7. Refractive indices and chromatic dispersions of polymers[a]

entry	polymer	$n_{632.8}$	ν_D	D
1	P**1a/2a/3a**	1.659	24.347	0.041
2	P**1a/2a/3b**	1.654	22.079	0.045
3	P**1b/2a/3a**	1.639	25.751	0.039
4	P**1c/2a/3a**	1.627	34.195	0.029
5	P**1a/2b/3a**	1.652	18.243	0.055
6	P**1a/2c/3a**	1.644	20.453	0.049
7	P**5**	1.635	28.788	0.035
8	P**6**	1.611	31.496	0.032
9	P**7**	1.606	47.155	0.021

[a] Abbreviation: n = refractive index, ν_D = Abbé number = $(n_D - 1)/(n_F - n_C)$, where n_D, n_F, and n_C are the n values at wavelengths of Fraunhofer D, F, and C spectral lines of 589.2, 486.1, and 656.3 nm, respectively; D = chromatic dispersion = $1/\nu_D$. The definition of ν_D and D can be found in literatures.[6]

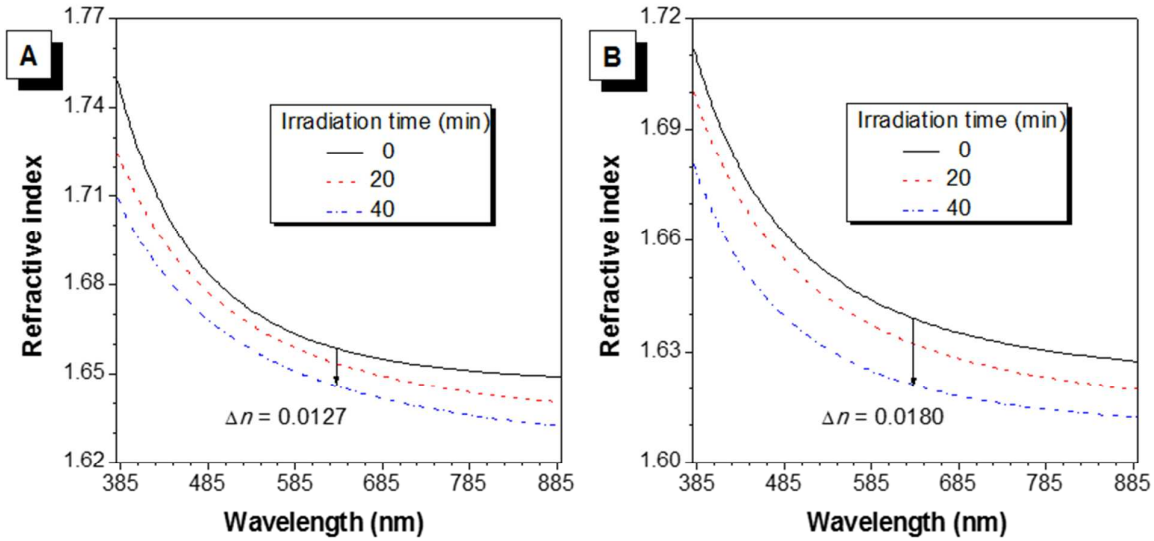

Figure S49. Wavelength dependence of refractive index of thin films of (A) P**1a/2a/3a** and (B) P**1b/2a/3a** at different UV irradiation time.

Table S8. Refractive indices and chromatic dispersions after UV irradiation for different time[a]

entry	polymer	t (min)	$n_{632.8}$	ν_D	D
1	P**1a/2a/3a**	0	1.659	24.347	0.041
2	P**1a/2a/3a**	20	1.654	25.302	0.040
3	P**1a/2a/3a**	40	1.646	26.498	0.038
4	P**1b/2a/3a**	0	1.639	25.751	0.039
5	P**1b/2a/3a**	20	1.632	25.852	0.039
6	P**1b/2a/3a**	40	1.621	31.305	0.032

[a] Abbreviation: t = UV irradiation time, n = refractive index, ν_D = Abbé number = $(n_D - 1)/(n_F - n_C)$, where n_D, n_F, and n_C are the n values at wavelengths of Fraunhofer D, F, and C spectral lines of 589.2, 486.1, and 656.3 nm, respectively; D = chromatic dispersion = $1/\nu_D$.

Reference

[1] a) H. Q. Wu, H. K. Li, R. T. K. Kwok, E. G. Zhao, J. Z. Sun, A. J. Qin, B. Z. Tang, *Sci. Rep.* **2014**, *4*, 5107; b) A. R. Katritzky, J. W. Rogers, R. M. Witek, A. V. Vakulenko, P. P. Mohapatra, P. J. Steel, R. Damavarapu, *J. Energ. Mater.* **2007**, *25*, 79.

[2] Y. Zhang, J. W. Y. Lam, B. Z. Tang, *Polym. Chem.* **2016**, *7*, 330.

[3] Y. Y. Zhao, C. Y. Y. Yu, R. T. K. Kwok, Y. L. Chen, S. J. Chen, J. W. Y. Lam, B. Z. Tang, *J. Mater. Chem. B* **2015**, *3*, 4993.

[4] (a) C. T. Lee, W. T. Yang, R. G. Parr, *Phys. Rev. B* **1988**, *37*, 785; (b) A. D. Becke, *J. Chem. Phys.* **1993**, *98*, 5648.

[5] Frisch, M. J.; Trucks, G. W.; Schlegel, H. B.; Scuseria, G. E.; Robb, M. A.; Cheeseman, J. R.; Scalmani, G.; Barone, V.; Mennucci, B.; Petersson, G. A.; Nakatsuji, H.; Caricato, M.; Li, X.; Hratchian, H. P.; Izmaylov, A. F.; Bloino, J.; Zheng, G.; Sonnenberg, J. L.; Hada, M.; Ehara, M.; Toyota, K.; Fukuda, R.; Hasegawa, J.; Ishida, M.; Nakajima, T.; Honda, Y.; Kitao, O.; Nakai, H.; Vreven, T.; Montgomery, J. A., Jr.; Peralta, J. E.; Ogliaro, F.; Bearpark, M.; Heyd, J. J.; Brothers, E.; Kudin, K. N.; Staroverov, V. N.; Keith, T.; Kobayashi, R.; Normand, J.; Raghavachari, K.; Rendell, A.; Burant, J. C.; Iyengar, S. S.; Tomasi, J.; Cossi, M.; Rega, N.; Millam, J. M.; Klene, M.; Knox, J. E.; Cross, J. B.; Bakken, V.; Adamo, C.; Jaramillo, J.; Gomperts, R.; Stratmann, R. E.; Yazyev, O.; Austin, A. J.; Cammi, R.; Pomelli, C.; Ochterski, J. W.; Martin, R. L.; Morokuma, K.; Zakrzewski, V. G.; Voth, G. A.; Salvador, P.; Dannenberg, J. J.; Dapprich, S.; Daniels, A. D.; Farkas, O.; Foresman, J. B.; Ortiz, J. V.; Cioslowski, J.; Fox, D. J. Gaussian 09, Revision D.01; Gaussian, Inc., Wallingford, CT, 2013.

[6] C. K. W. Jim, A. Qin, J. W. Y. Lam, F. Mahtab, Y. Yu, B. Z. Tang, *Adv. Funct. Mater.* **2010**, *20*, 1319.